LEVEL II

To be published in "Experimental Methods of Materials Science" Vol. I.

AD A060349

NORTHWESTERN UNIVERSITY

DEPARTMENT OF MATERIALS SCIENCE

(9) Technical Report, No. 21
September 26, 1978

(11) 26 Sep 78

(12) 113p.

(15) Office of Naval Research
Contract N00014-75-C-0580
NR 031-733

(14) TR-21

DDC FILE COPY

(6) THE MEASUREMENT OF RESIDUAL STRESSES BY X-RAY DIFFRACTION TECHNIQUES.

by

(10) M. R. James and J. B. Cohen

EVANSTON, ILLINOIS

78 10 19 042

TABLE OF CONTENTS

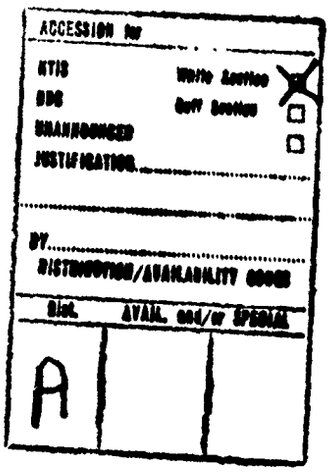

I. INTRODUCTION

The need to consistently monitor and preserve the strength characteristics of materials during manufacture and service, coupled with advanced design techniques utilizing a greater percentage of the available strength of such materials has necessitated rapid advances in the use of non-destructive testing, and characterization of residual stresses in particular. In response to this need important developments in equipment and measuring techniques and a greater understanding of the theoretical background have led to wider acceptance of the analysis of stress with x-rays, both as an experimental technique and as an engineering tool.

The idea of measuring residual stresses by x-ray diffraction was first proposed by Lester and Aborn (1925). The technique has long been used in the study of such manufacturing processes as shot peening, carburizing and heat treating. A bibliography on x-ray stress analysis prior to 1953 (Isenburger, 1953) lists 240 references, and this was before widespread use of the diffractometer. Only within the last few years, however, has the portability of the equipment and the rapidity of the technique been sufficient for its application to such areas as on-site inspection during fabrication, or in-field measurements for maintenance.

In this report the main aim is to present, in a single chapter, many of the recent instrumental advances and to explain the fundamental limitations associated with the measurement. This in the hope of providing an insight into its proper application. In doing so, many current applications are described in those areas where the measurement has already proven to be useful.

useful.

The International System of Units (SI) has been adopted. To obtain values in other units the following conversions will be helpful:

1 ksi (1000 lb/in^2) = 6.895 MPa (MN/m^2)

1 kg/mm^2 = 9.807 MPa

II. TYPES OF RESIDUAL STRESSES

The relevance of residual stress distributions to all major failure mechanisms, structural and dimensional stability, stress corrosion cracking and fatigue has been recognized for many years, but the actual extent of these stresses and their specific role is still sometimes uncertain in practice (Bunce, 1977). Nonetheless, a considerable number of reviews pertaining to the role and measurement of residual stresses exist (Baldwin, 1949; Rassweiller and Grube, 1959; Rimrott, 1962; Horger, 1965; Denton, 1966, 1971; McClintock and Argon, 1966; Air Force Materials Laboratory, 1976; Schmidt, 1976; and Parlane, 1977). Before describing the x-ray technique, a look at the definitions and general causes of residual stresses will be helpful.

Residual stresses are those stresses that are contained in a body which has no external traction (excluding gravity or another source such as a thermal gradient). Residual stresses belong to the larger group of internal stresses which apply to a body even while it is externally loaded. The two are often used interchangeably because both may be determined with x-ray diffraction, indirectly, from a measurement of the existing strains. To actually obtain the stress, a calculation is always necessary, which requires knowledge of elastic constants of the material or a calibration procedure. These often depend on the extent or range of the strain in question.

In the United States, residual stresses (strains)are classified into two types (Evans and Littman, 1963; ASTM (1977); Society of Automotive Engineers Handbook, 1978) "macro" and "micro" as shown in Table I. Researchers in other countries prefer to delineare three kinds of residual stresses (Wolfstieg and Macherauch, 1976; Buck and Thompson, 1977). The boundaries between any of these classifications are not sharply defined. These latter definitions are also given in Table I.

Table I

The first kind, termed macroscopic, is long range in nature extending over regions millimeters in dimension. Macro residual stresses and applied stresses add algebraically at least up to the elastic limit and are thus important in determining load carrying capabilities. These stresses may develop from mechanical processes such as surface working, forming and assembly, thermal processes such as heat treatments, casting and welding and chemical processes such as oxidation, corrosion and electro-polishing (Hilley et al., 1971). This class of stresses is measurable by mechanical means (by examining distortions after removing layers or boring, for example, often with strain gages) and also gives rise to shifts of peaks in an x-ray diffraction pattern.

The second kind of residual stress exists over dimensions of microns and is termed a microstress. It may be caused by yield anisotropy between grains or by a difference in the mechanical properties of different phases or regions in a material (such as the surface and the interior). While not detected by mechanical methods, these stresses give rise to both a peak shift and if they vary from point to point, line broadening in x-ray patterns. The third kind, which ranges over dimensions of 1 - 1000 Å, gives rise to x-ray line broadening only. These stresses arise

from the varying stress fields of individual dislocations, dislocation pile-ups, kink boundaries and other microstructural phenomena of a discontinuous nature. Actually, the magnitude of these stresses cannot be determined with x-rays, only their range or variance from Fourier analysis of diffraction peak.

In fatigue crack propagation and structural stability, bulk values, and therefore macro residual stresses, are the most significant. However, in both fatigue crack initiation and stress corrosion cracking (Hilley et al., 1971; Cathcart, 1976) all types of stress may be important depending on the situation. While the understanding of the effect of various types of residual stresses on performance may as yet be deficient, the potential exists for their proper evaluation, an important step in quantitatively assessing their role. The rest of this review is concerned with the x-ray techniques for doing this, and examples of their applications.

III. PRINCIPLES OF X-RAY STRESS MEASUREMENT

A. General Principles

The fundamentals of determining the surface residual stresses with x-ray diffraction have been derived in several sources (Barrett and Massalski, 1966; Hilley et al., 1971; Klug and Alexander, 1974; The Society of Materials Science, 1974; Hårterei Tech.-Mitt., 1976, Cullity, 1977). In this section the different methods are presented. In the following section, the instrumentation for the individual techniques is described.

Each form of identical planes of atoms in a polycrystalline material has an average interplanar spacing, $d_{hk\ell}$, which, when acted upon by an elastic stress, changes to a new value dependent on the direction and magnitude of that stress. A change, $\Delta d_{hk\ell}$, in the interplanar spacing will cause a corresponding change, $\Delta\theta$, in the Bragg angle of diffraction by the planes (Bragg's law: $\lambda = 2d\sin\theta$ where λ is the wavelength

of the incident x-rays). The strain $\Delta d/d$, can be measured by the change in the diffraction angle and the stress is obtained from the strain with formulae usually derived from linear isotropic elasticity theory.

Fig. 1

The principal stresses σ_1 and σ_2, (usually assumed to lie in the surface, but see Sec. V. C. 4), the general surface stress, σ_φ, and the corresponding strains are shown in Fig. 1. The term ψ is the angle between the surface normal and the direction of the strain being measured. The application of isotropic continuum elasticity theory to this problem yields the following relationship between the principal stresses in known directions, surface stress and measured strain, $\epsilon_{\varphi,\psi}$ (Hilley et al., 1971):

$$\epsilon_{\varphi,\psi} = \frac{1+\nu}{E}(\sigma_1\cos^2\varphi + \sigma_2\sin^2\varphi)\sin^2\psi - \frac{\nu}{E}(\sigma_1 + \sigma_2) = \frac{d_{\varphi,\psi} - d_o}{d_o}, \qquad (1)$$

where E is Young's modulus and ν is Poisson's ratio.* In this equation, $d_{\varphi,\psi}$ is the lattice spacing in the direction defined by φ and ψ (see Fig. 1) and d_o is the interplanar spacing of the stress free state.

The component of stress in the surface at the angle φ, σ_φ, is given by:

$$\sigma_\varphi = \sigma_1\cos^2\varphi + \sigma_2\sin^2\varphi. \qquad (2a)$$

Also:

$$-\frac{\nu}{E}(\sigma_1 + \sigma_2) = \frac{d_{\varphi,\psi=0} - d_o}{d_o}. \qquad (2b)$$

Substitution of these equations into Eq. 1 yields:

$$\frac{1+\nu}{E}\sigma_\varphi\sin^2\psi = \frac{d_{\varphi,\psi} - d_{\varphi,\psi=0}}{d_o} \cong \frac{d_{\varphi,\psi} - d_{\varphi,\psi=0}}{d_{\varphi,\psi=0}}. \qquad (3)$$

The replacement of d_o by $d_{\varphi,\psi=0}$ in the denominator leads to errors of $\approx$ 1-2 MPa, well within uncertainty in the measurement (see Chap. IV). This step eliminates the need to know the stress free interplanar spacing: only the stressed specimen needs to be examined.

*In the German literature $(1+\nu)/E$ is written as $\frac{1}{2}s_2(hk\ell)$ and $-\nu/E$ as $s_1(hk\ell)$.

Equation 3 forms the basis of the analysis by relating a measurable change in the interplanar spacing, $\epsilon_{\varphi,\psi}$ to the surface stress. Fig. 2a illustrates how this measurement is achieved. A stress will cause the interplanar spacing of grains oriented at various angles to the surface to be different. The interatomic spacing becomes the gage length. Variation of this gage length with orientation of the specimen, ψ, can be determined by three principle methods: the $\sin^2\psi$, two-tilt and single-tilt techniques.

Fig. 2

1. $\underline{\text{Sin}^2\psi \text{ Method}}$

In this method several values of lattice strain are measured, each at a different ψ tilt of the specimen. It is then possible to determine the surface component of stress from a least-squares straight line for the lattice strain as a function of $\sin^2\psi$. The stress is measured along the direction of the intersection of the ψ tilt and the specimen (Fig. 2c). Now, let:

$$m^* = \frac{\partial \epsilon_{\varphi,\psi}}{\partial \sin^2\psi} . \tag{4a}$$

Therefore:

$$\sigma_\varphi = \frac{m^*}{(\frac{1+\nu}{E})} . \tag{4b}$$

In terms of the quantity usually determined, the interplanar spacing, it follows that with:

$$m' = \frac{\partial d_{\varphi,\psi}}{\partial \sin^2\psi} , \tag{5a}$$

then:

$$\sigma_\varphi = \frac{m'}{d_{\varphi,\psi=0}\ (\frac{1+\nu}{E})} . \tag{5b}$$

Because several values of $d_{\varphi,\psi}$ are determined, errors resulting from random fluctuations are minimized. Four to six ψ tilts, taken in equal increments of $\sin^2\psi$, are normally employed.

2. 'Two Tilt' Method

Isotropic elasticity theory predicts that the strain $\epsilon_{\varphi,\psi}$ is linearly dependent on $\sin^2\psi$, as was shown in Eq. 3. When this holds true (see Chap. V) only two inclinations of the sample are necessary to determine the surface stress. The interplanar spacings are determined at $\psi = 0$ and at an inclination of $\psi = \psi$. The formula relating the stress to the strain is then given by:

$$\sigma_{\varphi} = \left(\frac{E}{1+\nu}\right) \cdot \frac{1}{\sin^2\psi} \cdot \frac{d_{\varphi,\psi} - d_{\varphi,\psi=0}}{d_{\varphi,\psi=0}} \quad (6)$$

The term $(E/1+\nu)\cdot 1/\sin^2\psi$ is often combined into a calibration constant, K, which can be experimentally determined for a particular combination of ψ and reflecting planes in a given material. Experimental determination of K is desirable because bulk values of E and ν are not necessarily applicable (Klug and Alexander, 1974). The equations which have been presented are based upon isotropic elasticity while most crystalline materials show elastic anisotropy. The measured strains which correspond to one particular crystallographic direction cannot be accurately related to stress by mechanically measured values of the bulk elastic constants (Bollenrath, Hauk and Müller, 1967). In addition, the effective values of E and ν are influenced by interactions between a grain and its surroundings (Greenough, 1952) by plastic deformation (Taira et al., 1969), by preferred orientation (Shiraiwa and Sakamoto, 1970) and by the presence of second phase particles (Shiraiwa and Sakamoto, 1970). While some of the interactions have been studied theoretically (see Sec. V.B.) the elastic constants measured by x-rays are preferrable over

theoretically deduced or mechanically measured values. The experimental procedures for such a determination are included in most review articles (Barrett and Massalski, 1966; Klug and Alexander, 1974; The Society of Materials Science, Japan, 1974, Hauk and Wolfstieg, 1976; Cullity, 1977). These consist essentially of subjecting a piece of the material to a known elastic load, and measuring the shift of the diffraction peak from the {hkℓ} planes in question.

It is unfortunately common practice to replace $(d_{\varphi,\psi} - d_{\varphi,\psi=0})/d_{\varphi,\psi=0}$ in Eq. (6) by the approximation $-\cot\theta \cdot \frac{1}{2}(2\theta_o - 2\theta_\psi)$, obtained by differentiating Bragg's law, to obtain a formula in terms of the peak position 2θ:

$$\sigma_\varphi = \tfrac{1}{2} \cdot \frac{\pi}{180} \cdot \left(\frac{E}{1+\nu}\right) \cdot \frac{1}{\sin^2\psi} \cdot \cot \tfrac{1}{2}(\theta_o + \theta_\psi) \cdot (2\theta_o - 2\theta_\psi) , \quad (7)$$

where $2\theta_o$ and $2\theta_\psi$ are in degrees. This substitution introduces appreciable error, if the stress is large. The stress constant becomes:

$$K = \frac{1}{2} \cdot \frac{\pi}{180} \cdot \left(\frac{E}{1+\nu}\right) \cdot \frac{1}{\sin^2\psi} \cdot \cot \tfrac{1}{2} (\theta_o + \theta_\psi), \quad (8a)$$

and:

$$\sigma_\varphi = K \, \Delta 2\theta. \quad (8b)$$

Inexpensive micro- and mini-computers are readily adopted to on-line data processing in this kind of study, and such simplications are really no longer necessary.

3. 'Single Exposure' Method

A stress component may be measured from a single inclination if the Bragg angle is determined at two positions on the diffraction cone from a polycrystalline specimen. Fig. 3 depicts the geometry in which all the crystallites which are favorably oriented with respect to the incident beam diffract forming a cone of radiation (the Debye cone). The incident x-ray beam is directed toward the specimen surface at a fixed angle β from the surface normal, and the

Fig. 3

angle of the plane normals corresponding to the two measuring directions are η_1 and η_2. If one measures the Bragg angle at two positions on the cone by recording the cone on film (B and C in Fig. 3) the corresponding tilt angles are $\psi_1 = (\beta - \eta_1)$ and $\psi_2 = (\beta + \eta_2)$. The diffraction ring will be asymmetric if the interplanar spacings of the diffracting crystallites are different as a result of residual strains.

From Eq. (6) an equation relating d_1 to ψ_1 and one relating d_2 to ψ_2 can be written. Combining the formulae and writing the d spacings in terms of the Bragg angle, the stress is given by (Hilley et al., 1971):

$$\sigma_\varphi = \frac{E}{1+\nu}\left[\frac{\cot \tfrac{1}{2}(\theta_1+\theta_2)}{\sin^2(\beta+\eta)-\sin^2(\beta-\eta)}\right](\theta_2 - \theta_1), \tag{9}$$

where $\eta_1 = (90^\circ - \theta_1)$ and $\eta_2 = (90^\circ - \theta_2)$. Also, in the trigonometric terms in the denominator, it is assumed $\eta_1 \simeq \eta_2 \simeq \eta$. Writing the Bragg angle in degrees and noting $\eta = 90-\theta^\circ$:

$$\sigma_\varphi = \frac{\pi}{180}\frac{E}{1+\nu}\left[\frac{\cot \tfrac{1}{2}(\theta_1+\theta_2)}{2\sin 2\beta \cos\theta \sin\theta}\right](\theta_2 - \theta_1). \tag{10}$$

The formula is often written in terms of a stress constant:

$$\sigma_\varphi = K\Delta\theta, \tag{11a}$$

where:

$$K = \frac{\pi}{180}\cdot\frac{E}{1+\nu}\cdot\frac{1}{2\sin 2\beta \sin^2\theta}. \tag{11b}$$

[As in Eq. (8) it is assumed in Eq. (11) that $\cot \tfrac{1}{2}(\theta_1+\theta_2) \simeq \cot\theta$.]

If the recording of the diffraction ring is made on film, the Bragg angle need not be explicitly calculated. Relations in terms of the sample to film distance, R, and S_1 and S_2, the measured distances along the film from the axis of the incident beam to the center of the diffraction maxima

may be used. For a flat film the relation is:

$$\sigma_{\varphi} = K^{*}(S_2 - S_1), \tag{12a}$$

where

$$K^{*} = \left(\frac{E}{1+\nu}\right)\left[1/(f\ R\sin^2 2\beta \sin^2\theta)\right]. \tag{12b}$$

In actual practice, the distance S may be measured from some sort of fiducial mark that is recorded on the film a fixed distance from the beam axis or from the peaks of a stress free powder dusted on the surface. A detailed derivation of the appropriate formula and pertinent techniques is given in Norton (1967) and Kraus and Nehasil (1976). Such film techniques are becoming less popular as the portability of diffractometers increases (see Sec. III. B. 4) as they are inherently less accurate and precise. As seen from Eqs. (8) and (11) the residual stress is related to the peak shift, $\Delta\theta$, by a stress constant. A plot of the stress constant for iron as a function of θ in the back-reflection range 75° - 88° is given in Fig. 4. In the case of the 'single exposure' method, curves are plotted for typical values of $\beta = 35^{\circ}$ and 45° while for the 'two tilt' method the curves are for the typical ψ angles of 45° and 60°. An inspection of these curves shows that while the stress constant is almost independent of θ for the 'single exposure' method it is 1½ to 3 times greater than the stress constant in the 'two tilt' technique at the important angles of 78° and 80.5°.* From the viewpoint of inherent sensitivity, the smaller stress constant would require a large peak shift for the same stress (Eqs. (8) and (11)) so that the 'two tilt' method should be superior. Norton (1967) claimed that this advantage is difficult to achieve

Fig. 4

*These angles correspond to the CrK_{α} 211 and CoK_{α} 310 diffraction lines from Fe.

because alignment of the specimen is more critical in the two tilt method. But recently it has been shown that the two tilt method is not as susceptible to sample displacement as was previously believed (James and Cohen, 1977) (see Sec. III. B. 3). In the most favorable cases errors as low as $\pm$ 14 MPa ($\pm$ 2 ksi) can be obtained (in the two-tilt procedure) but errors of double to triple this amount may occur in less favorable cases (Andrews et al., 1974) (see Chap. IV).

4. Determining the Stress Tensor

Finally, it should be mentioned that the principal stresses (and their direction can be obtained from several such stress measurements at different φ and ψ angles (Schaaber, 1939; Macherauch and Muller, 1961; Stroppe 1963; Barrett and Massalski, 1966; Peiter, 1976; Dölle and Hauk, 1976). In these references various assumptions are made about the terms in the stress tensor, except for the latest papers. Some of these more recent methods involved knowing the "d" spacing of the unstressed state, which is difficult in view of the effects of sample displacement on 2θ (Sec.IV.B.3). If considerable care in the measurement is possible these do look promising. The last two references in particular allow one to examine the entire stress tensor σ_{ij}.

In particular, the shear stress normal to the sample's surface and the normal stress should be zero if the stress state is truly two dimensional, but in some cases this has been found not to be the case (see Sec.V. C. 4).

The method of Dölle and Hauk (1976) for this purpose will be explained briefly. The analysis is based on strains (ε_{ij}) and primes imply values in laboratory coordinates, whereas unprimed quantities

refer to the specimen axes. For example, ϵ'_{33} is the strain normal to the diffracting planes:

$$\epsilon'_{33}(\varphi,\psi) \equiv \frac{d_{\varphi,\psi} - d_o}{d_o} = \epsilon_{33}[\epsilon_{11}\cos^2\varphi + \epsilon_{12}\sin 2\varphi + \epsilon_{22}\sin^2\varphi - e_{33}]\sin^2\psi +$$

$$[\epsilon_{13}\cos\varphi + \epsilon_{23}\sin\varphi]\sin 2\psi \qquad (13)$$

By adding eq. (13) for $+\psi$, $-\psi$ a quantity (a_1) is formed. The value of a_1 at $\psi = 0$ yields ϵ_{33}, and $\partial a_1 / \partial \sin^2\psi$ yields $\epsilon_{11} - \epsilon_{33}$ for $\varphi = 0$ (and hence ϵ_{11}) and for $\varphi = 90^\circ$, $\epsilon_{22} - \epsilon_{33}$. The value of ϵ_{12} results from measurements at $\varphi = 45^\circ$. Taking the difference of Eq. 13 for $+\psi$, $-\psi$ (a_2):

$$\frac{\partial a_2}{\partial \sin 2\psi} = \begin{cases} \epsilon_{13} \text{ for } \varphi = 0. \\ \epsilon_{23} \text{ for } \varphi = 90^\circ. \end{cases} \qquad (14)$$

From the strains, the stresses are obtained from:

$$\sigma_{ij} = \frac{E}{1+\nu}\left[\epsilon_{ij} + \frac{\nu}{1-2\nu}\delta_{ij}(\epsilon_{11} + \epsilon_{22} + \epsilon_{33})\right] \qquad (15)$$

Where δ_{ij} is the Kronecker delta (equal to zero unless $i = j$), and x-ray values of the elastic constants are employed. The magnitudes and directions of the principal stresses can then be obtained by standard tehcniques of matrix transformation.

These methods of residual stress measurement by x-ray diffraction are derived from isotropic elasticity theory and assume homogeneous deformation. They have been shown in certain special cases to deviate from the predictions of this theory particularly when applied to samples which have been plastically deformed severely enough to cause strong changes in texture along with the stress (not just texture prior to producing a stress) (Macherauch, 1961; Donachie and Norton, 1961; Ricklefs and Evans, 1966; Wiedemann, 1966; Bollenrath et al., 1967; Shiraiwa and Sakamoto, 1971; Marion, 1972; Marion and Cohen, 1974). Such problems are discussed in Sec. V.C.

B. Equipment and Methods of Analysis

1. Introduction

It should be clear that residual stress measurements are in reality precise measurements of the lattice strain between specially oriented crystallographic planes. There are a variety of experimental procedures capable of determining these strains. Their relative merits and problems are discussed in this section. A brief description of the avaialble equipment is also given.

The many different types of instrumentation all employ one common feature in determining the position of a diffraction peak: high angle (back reflection) diffraction lines are used, to increase the accuracy. As can be seen from Eq. (7) a given stress level will produce a larger shift of the diffraction lines as the θ angles approach 90°. Also, the absolute peak position is less sensitive to sample displacement in the back reflection region. Common crystallographic planes and their diffraction angle for different radiations may be found in many references (Barrett and Massalski, 1966; Hilley et al. 1971; Klug and Alexander, 1974; The Society of Materials Science, Japan, 1974; Cullity, 1977). For steel with CrK_{α} radiation and the 211 peak there is a shift between the $\psi = 0$ and $\psi = 60^{\circ}$ peaks of $\approx 0.1^{\circ}$ for each ≈ 40 MPa. Shifts of $\pm$ 0.01 - 0.02° can be readily detected.

2. Film Techniques

As mentioned in the previous section the use of the photographic method has declined recently but it still possesses some advantages: a) becuase the entire diffraction cone is observed added information can be obtained on grain size, extent of cold work and heat treatment, and preferred orientation; b) the film method requires simple instrumentation (Bolstad and Quist, 1965), but processing of film and determining the diffraction profiles requires much longer experimental time than with counter methods. This extra time may be reduced with instant-processing film and direct reading by microphotometry but no such

manufactured stress measurement device is available yet.

Film techniques can employ both the single exposure and the two-tilt methods (Macherauch, 1961; Norton, 1967; Hawkes, 1970; Andrews et al., 1974). The relative merits and individual problems of each method must be taken into account (see Sec. III. A. 3.).

3. Diffractometer Techniques

The diffractometer methods utilize an x-ray detector (scintillation or proportional counter) to quantitatively record the intensity profile. The detector moves 2θ while the sample moves θ to maintain good focusing as described in (a) below. In addition, the specimen holder must be able to rotate independently of the detector motion so that the lattice strain can be determined at various ψ angles. Sample oscillation or rotation will help if the grain size is too coarse (greater than a few tenths of a millimeter). This oscillation is possible on diffractometers in which the θ and 2θ drives can be operated independently; but when these drives are coupled separate rotary motions must be supplied for setting the ψ inclination as well as for oscillation. Other than this limitation any diffractometer may be used for stress measurements in the laboratory.

For many years, the classical Bragg-Brentano diffractometer ("Ω-diffractometer") was the most common instrumental arrangement. While still in heavy use in the United States, it is being superceded by the "ψ-diffractometer" in Germany and Japan. The former arrangement will be discussed first.

a. Ω-Diffractometer

In the Bragg-Brentano or Ω-diffractometer (also referred to as a para-focusing diffractometer) the x-ray source, F, specimen, S, and counter, C,

Fig. 5 C, all lie in the equatorial or focusing plane shown in Fig. 5. The geometrical arrangement on a focusing circle of diverging source, sample and detector causes the diffracted rays from a form of planes {h k ℓ} to converge at a single point. The counter pivots about the goniometer axis, i.e., about an axis perpendicular to the equatorial plane. As C pivots about S, the focusing circle changes radii (as seen in Fig. 5) and the specimen must be rotated at one-half the angular velocity of the detector to maintain focus. The ψ angle is obtained by rotating the specimen on the goniometer axis independently of the counter. As seen in Fig. 6 this pro-

Fig. 6 duces a new focal point. In actuality, the focus is not perfect because the specimen is generally flat rather than curved to fit the focusing circle, and from the three-dimensional properties of the system (finite dimensions of the sample, source and receiving slit). However, in order to achieve the best possible focusing during the ψ inclination, the receiving slit and/or detector must be moved, to point C in Fig. 6b, the new focal point.

The motion of the receiving slit must be truly radial or an error will occur (because the $0^{o}2\theta$ position will have changed). This movement is neglected in the so called stationary slit technique; the receiving slit and detector remain on the goniometer circle of Fig. 6 at all times, deliberately not fulfilling focusing conditions. A sacrifice in intensity is made but the complication of moving the receiving slit is avoided. An excellent study of the geometric errors associated with each method has been presented by Zantopulos and Jatczak (1970). They conclude that the lack of focusing in the stationary slit technique does not introduce significant error in determining the peak shift. James (1977) has studied the

repositioning of the receiving slit using a sturdy worm gear and dovetail slide. This system introduced an average error of about $\pm$ 4 MPa over the stationary slit method on a steel sample with a compressive stress of 164 MPa. Other less perfect systems involving manually repositioning the slit are likely to introduce even larger errors.

The Japanese (Taira et al., 1969) have adopted a non-focusing technique called the parallel beam procedure and applied it to the Bragg-Brentano arrangement. Using long Soller baffles or plates perpendicular to the diffractometer plane (rather than in the usual position parallel to it) the x-rays form a highly collimated parallel beam. The angle of diffraction is uniquely defined by the angle between the primary and diffracted beam soller plates, Fig. 7, and a receiving slit is not necsary.

Fig. 7

Each of the these optical arrangements, the parafocussing, stationary-slit, and parallel beam techniques have a different inherent sensitivity to sample displacement. If the sample is displaced from the center of the diffraction circle, as in Fig. 8, there is a relative shift of the diffracted rays between $\psi = 0^{\circ}$ and $\psi = \psi^{\circ}$. This has been examined by Cohen (1964) and French (1969). Denoting ΔX as the displacement, the equation for the error in peak shift at two tilts in degrees 2θ, is:

Fig. 8

$$\delta(\Delta 2\theta)_{SD} = \frac{360}{\pi} \Delta X \cos\theta \left[\frac{1}{R_{GC}} - \frac{\sin\theta}{R_p \sin(\theta+\psi)}\right], \qquad (16)$$

where R_p represents the distance from the sample at the focus position; it is given by (Hilley et al., 1971):

$$R_p = R_{GC} \frac{\cos(\psi + (90-\theta)}{\cos(\psi - (90-\theta)}, \qquad (17)$$

where R_{GC} is the goniometer radius. In the parallel beam technique, the angular relationship depends solely on the angle between the parallel soller baffles, and not on the position of the sample, eliminating this error due to sample displacement.

Equation (16) has been experimentally verified (James and Cohen, 1977) together with the fact that the parallel beam procedure is insensitive to sample position. Most interesting, however, is the fact that because R_p is constant in the stationary slit method, ($R_p = R_{GC}$) this technique is approximately 5 times less sensitive to sample displacement than parafocussing geometry while producing a sharper and more intense diffraction profile than the parallel beam method. Hence a peak can be located (to the same precision) more quickly with the stationary slit technique than with a parallel beam.

b. ψ-Diffractometer

Stress measurements may also be made on a "ψ-diffractometer," where the specimen is rotated around an axis lying parallel to the diffractometer plane, i.e. normal to the goniometer axis, as in Fig. 9. This geometry,

Fig. 9

similar to the Schulz method (1949) for pole figure determination, was first applied to stress measurements by Wolfstieg in 1959 and has become popular in Europe during recent years. The principle characteristics and applications have been summarized by Macherauch and Wolfstieg (1977). Often referred to as the "side inclining procedure," its unique advantage lies in the fact that there are equal path lengths for the incident and diffracted rays independent of θ, ψ and the vertical divergence. During rotation of the specimen around the ψ axis, the x-ray tube, specimen surface and counter all remain on the focusing circle eliminating the relocation of the receiving slit to obtain optimum focusing. As the path length for incident and scattered beams inside the specimen

is the same there is no need for an absorption correction after a ψ-tilt as there is for the Ω diffractometer (see Sec. IV. B. 1.).

As seen in Fig. 9, a horizontal slit is used to control the divergence of the x-ray beam in the vertical direction which reduces the intensity. However, in many instances, further use of Soller slits to control divergence is unnecessary (The Society of Materials Science, Japan, 1974). The intensity is also lowered, however, due to misfocus above and below the ψ-axis due to the height of the beam. In implementing this technique on a Bragg-Brentano diffractometer, great care must be taken to place the incident beam symmetrically about the ψ axis, or errors in peak location will result. Such instrumental factors have been studied (Yoshioka, 1976, Macherauch and Wolfstieg, 1977).

This method is particularly useful with specimens of complex shape such as the flank of a gear tooth or at the corner of a structure. In such cases, the incident or diffracted ray may be blocked by the specimen at one ψ angle or another in the older technique.

c. Computer Controlled Diffractometers

Since the appearance of inexpensive minicomputers and dedicated microprocessing systems, computer controlled diffractometers are more prevalent in x-ray laboratories. Such instrumentation lends itself very nicely to the measurement of residual stress. Manual measurements on a diffractometer requires accumulating x-ray counts at individual settings across the diffraction profile at each ψ inclination, a tedious and time consuming procedure. Hardware-controlled step scanning may save operator time but is of limited value since the peak position and breadth varies with sample,

residual stress level and ψ angle. Indeed, the need for operator control has probably been the chief reason for the proliferation of the 'two tilt' method over the '$\sin^2\psi$' method, although more precision is obtained in the same time with the latter (James and Cohen, 1977) in an automated system.

Early automated systems (Koves and Ho, 1964; Crisci, 1972) required the collection of many data points due to the lack of on-line controls for locating the peak. Kelly and Eichen (1973) designed a system for the 'two tilt' method allowing for a three point parabolic fit to determine the peak position. Hayama and Hashimoto (1975) employ the parallel beam technique and define the peak as the midpoint of the breadth of the profile at half the maximum intensity. Both use counting statistics to determine the statistical error in a stress measurement.

Greater flexibility of operation has been achieved by the authors (James and Cohen, 1977) by providing a package capable of using either the 'two tilt' or '$\sin^2\psi$' technique, stationary slit or parafocusing geometry and sample oscillation. Also, if d vs $\sin^2\psi$ is not linear a method is implemented to obtain the true macrostress (see Sec. V. C). The system can be employed using a normal detector with or without movement of the receiving slit or with a one-dimensional position sensitive detector. Time is optimized by accumulating data to an operator specified total error (statistical plus geometric). Sample alignment is also automated. The peak is found automatically.

This kind of system is especially advantageous when many measurements are required such as in studies of fatigue (Quesnel et al., 1979) when many samples or test conditions must be examined.

The basic precision of the conventional diffractometer is ± 14 MPa (± 2 ksi) (Jatczak and Boehm, 1973) with measurement times of ≈ 45 minutes with manual operation, 15-20 minutes or less per specimen with a normal detector and automation, or 5 minutes with a position sensitive detector (see Chap. IV). However, the time of measurement, cost, lack of portability, and restriction on specimen size often limit the use of these laboratory instruments.

4. Portable Systems

. The need for both greater speed and transportability has promoted rapid development of x-ray stress analyzers over the last 10 years. At first this development has been based on modifications and innovations associated with or built around a diffractometer. The Japanese have been especially proficient in designing mobile diffractometers (Kamachi, 1971; Kamachi and Kawabe, 1976; Chrenko, 1977). One of these is portable. These are capable of scanning only in the high angle region. For stress measurements these instruments offer parallel beam geometry and either the standard or side-inclination method. A segment of a diffractometer is usually mounted at the end of a boom which is fixed to a wheeled platform or it can be magnetically attached to the structure being measured (Kamachi and Kawabe, 1976). These devices allow measurements on large-grained materials by oscillating the x-ray head about a mean ψ angle so that more grains can contribute to the diffracted intensity. Measuring times are of the order of 5-15 minutes.

Another instrument with the registered trademark, "Fastress," is based on a design by Weinman et al., (1969). This unit utilizes two x-ray tubes and two pairs of movable detectors to locate the peak, one pair of detectors at $\psi = 0^{\circ}$ and one pair at $\psi = 45^{\circ}$. Both peak positions are

found by matching the intensity in each detector with its mate, which is positioned on the other side of the profile. The midpoint between the two detectors is defined as the peak location. The method assumes the diffraction profile is symmetric and that detector efficiencies are matched. Reproducibility is about $\pm$ 20 MPa in a 3-minute measurement on hardened steel samples. The device is semi-portable in that the measuring head (incorporating the x-ray tubes, detectors and 2θ motion), electronics and power supply may be rolled on a cart in the laboratory. An example of its use in obtaining two-dimensional residual stress contours is the study by Catalano (1976).

A recent development called PARS (Portable Analyzer for Residual Stresses) involves the use of a position sensitive detector (PSD) (Borkowski and Kopp, 1968) and a miniature air cooled x-ray tube (James and Cohen, 1976; James and Cohen, 1978). The PSD replaces the counter and the diffractometer arrangement by simultaneously detecting the diffracted photons over a wide 2θ range yielding information on both the quantity and relative position of the incoming photons.* The quantitative information processed by the PSD electronics can then be projected onto a calibrated screen or fed directly to a computer to numerically locate the peak and calculate the stress.

The advantages of the PSD are two-fold: 1) it eliminates the need for bulky, heavy and expensive gearing and drive mechanisms characteristic of the conventional diffractometer and 2) it provides quantitative data

*The positional information is obtained electronically by examining the differences in shape of a pulse travelling to the two ends of the central wire in the detector.

simultaneously over a wide range ($\sim 20^{\circ}2\theta$, if necessary) enabling rapid accumulation and fast data processing.

The accuracy of stress measurements with such a portable unit has been evaluated by James and Cohen, (1978); the stress could be measured to $\pm$ 35 MPa or better in 4 to 20 seconds, depending on the specimen, and all from an apparatus that can be carried by one person, as the measuring head weighs 7-11 kg. It employs stationary slit geometry (to minimize sensitivity to positioning) and the two tilt technique. In Fig. 10 the device is shown in use hanging from a strap around the neck of one of the authors. A portable unit incorporating a PSD, but employing a normal water cooled x-ray tube is available from CGR in France, but measuring times are quite long in comparison to the above unit. It employs the single exposure technique which is inherently less precise than the other methods (Sec. III. A. 3). Another portable system is under development by Steffan and Ruud (1978). It employs fiber optics and therefore can be placed in pipes, etc. Measurements take $\approx$ five minutes.

Fig. 10

[Additional uses of the PARS device are possible. As the entire peak shape is recorded, the breadth of the diffraction profile can be determined. This can be useful in view of known empirical relationships between this quantity and hardness (Marburger and Koistinen, 1961). Because of the wide angular range covered by the detector, peaks from two phases could be examined and/or the quantity of retained austenite could also be determined at the same time.]

5. Other Techniques

There have been other techniques for stress analysis by x-ray diffraction (Keng and Weil, 1971; Hearn, 1977; Rozgonyi and Ciesielka, 1975; Wolfstieg, 1976; Mitchell, 1977; Barrett and Predecki, 1976; Barrett, 1977; Nagao and Kusumoto, 1976; Leonard, 1973) to examine specific problems. While not in general use, they illustrate the range of possibilities of the x-ray method. Keng and Weil (1971) present a technique for determining stresses in single crystals and Rozygonyi and coworkers (1973),

1976) and Hearn (1977) apply x-ray topography to the measurement of stress in thin films. Weissmann and Saka (1977) employ a similar technique for examining strains in notched and smooth silicon crystals. Berg and Hall (1975) employ divergent beam (pseudo Kossel) patterns to measure strain down to 2×10^{-5} in perfect silicon crystals. These techniques may be of particular interest in the electronics industry where such perfect crystals are common. As the main theme of this review is x-ray techniques applicable to most engineering situations, only two of these other techniques will be discussed in detail; stress measurements in polymeric materials and the use of polychromatic radiation.

Barrett and Predecki (1976) and Barrett (1977) have described a technique to measure applied and residual stresses in polymeric materials. By imbedding stress free metal particles into homogeneous or reinforced polymers, intense high angle diffraction lines suitable for stress measurement can be obtained. The time of measurement is fast enough to detect relaxation effects. The method can also be applied to unidirectional fiber reinforced samples. The applications mentioned by the authors refer not only to surface stresses but also to those at some depth below the surface.

Another technique based on the use of polychromatic radiation rather than the characteristic lines from an x-ray tube appears to lend itself to the construction of a simple measurement system. The possibility of such a system has been confirmed by Nagao and Kusumoto (1976) but suffers from a problem of precision (James, 1977; Leonard, 1973) ($\pm$ 70 MPa). To see why we will discuss the principles of this method.

It is based on the ability of a solid state detector (SSD) to analyze the energies of radiation. Because of its excellent energy

resolution ($\sim$ 170 eV) a SSD has been used recently for energy dispersive fluorescence studies, determining the elemental constituents of a specimen by analyzing the energy of photons emitted from the sample surface. It is also possible to use a SSD for 'energy powder patterns' as described by Giessen and Gordon (1968). Photons of different energies are diffracted at a fixed angle from different planes on a sample exposed to a continuum of radiation.

The ability to obtain the peaks in energy without having to scan the detector appears to simplify the method of residual stress analysis (as did the PSD).

Rewriting Bragg's law in terms of energy:

$$\lambda = 2d\sin\theta,$$

and:

$$U \equiv hc/\lambda,$$

so that:

$$U\sin\theta = hc/\lambda = 6195 \text{ (eV) } (\text{Å}), \qquad (18)$$

where U is in eV, d in Å and h and c are Planck's constant and the speed of light respectively. Residual stress changes the d spacing of the crystallites at $\psi = 0$ and at $\psi = \psi^{o}$ which results in photons of different energies being diffracted at each tilt. By measuring the peaks in energy at $\psi = 0^{o}$ and at an inclination, $\psi = \psi^{o}$, the energy shift of one peak can be determined. To determine a typical magnitude of this shift, the stress in the two-tilt method can be expressed as follows:

From Eq. (6):

$$\sigma_{\varphi} = \left(\frac{E}{1+\nu}\right) \frac{1}{\sin^{2}\psi} \frac{d_{\varphi,\psi} - d_{o}}{d_{o}} . \qquad (19)$$

Substituting in Eq. (18):

$$\sigma_{\varphi} = \left(\frac{E}{1+\nu}\right)\left(\frac{1}{\sin^2\psi}\right)\left(\frac{U_o - U_{\varphi,\psi}}{U_{\varphi,\psi}}\right) . \qquad (20)$$

Using elastic constants for steel of E = 207 GPa (30 x 10^6 psi), ν = .33 and a tilt of $\psi = 45^o$ the resultant energy shift for a stress of -70 MPa (-10152 psi) is $(U_o - U_{\varphi,\psi})/U_{\varphi,\psi} = 2.22 \times 10^{-4}$. For x-rays of energies $\approx$ 6 keV (the characteristic lines of Cr, for example) this implies an energy change of 1.3 eV, a very small shift to determine with a SSD having a resolution width at $\approx$ 6 keV of 170 eV. If it is assumed that the peak shift can be determined only to 5 eV, U must be near 25 keV. Such energies can be obtained using the white radiation of an x-ray tube rather than the spectral lines and the simplicity of the experiment is enhanced since the diffraction angle need not be known or scanned. However, there is a drastic decrease in intensity. Cole (1970) has derived an expression for the total diffracted power from a flat powder sample as:

$$P' = P(\lambda_{hk\ell})\left(\frac{e^4}{m^2c^4}\right)\frac{m}{16\pi R v_a^2}\frac{\lambda^4 F^2}{2A}\left(\frac{1+\cos^2 2\theta}{2\sin^3\theta}\right), \qquad (21)$$

where P' is the power per unit length of the diffracted cone, m, the multiplicity of the powder line, R, the sample-to-detector distance, and λ and A are the wavelength and absorption coefficient of the specimen for the diffracted phonon. If there are no absorption edges, A depends on λ^3 (Cohen, 1966) and therefore the diffracted power falls roughly as λ. Also in the structure factor, F, the term involving the Debye-Waller factor ($e^{-B\sin^2\theta/\lambda^2}$) falls as e^{-1/λ^2}. For energies of 25 keV ($\lambda \sim .5$ A) the total diffracted power will be very small. Thus, the resolution of the SSD limits the accuracy of a residual stress measurement made in a reasonable time because high energy x-rays are

necessary. Also for high energies, the peaks of interest occur at low angles, increasing the effects of sample displacement. For actual tests of the technique see Leonard (1973).

The technique has been applied (Nagao and Kusumoto, 1976) with a rotating anode x-ray generator to produce intense white radiation. The $\sin^2\psi$ method of stress analysis was adopted rather than the two-tilt method of Eqs. (20).

C. Summary

Diffractometers and film diffraction techniques with back reflection cameras may be used to determine the lattice spacing, d, or peak position, 2θ, at the appropriate ψ inclinations of the specimen for determining stresses. The diffractometer method is capable of full automation to reduce the tedious nature of repetitive measurements.

The limited size of specimens which can be measured on a diffractometer has led to the development of portable systems. The evolution of such devices has progressed from diffractometers on dollys to the use of position sensitive detectors and miniature x-ray sources, eliminating the mechanized scanning of the diffraction profile. These "state of the art" instruments increase the potential applications of residual stress measurement; results can be obtained in 4-20 seconds.

IV. CONTROL OF ACCURACY AND PRECISION

A. Introduction

This chapter will be concerned with precision in repeated stress measurements, and bias, that is possible differences between the mean of such repititions and the true value. The most important individual errors have received attention in the literature. An outline is presented here of the source and

magnitude of each contributing factor for the omega diffractometer.

B. Factors Influencing Bias in the Measurement

There are three broad categories into which all factors influencing the bias can be classified: instrumental, geometrical and specimen factors. A detailed list first compiled by Jatczak and Boehm (1973) is summarized in Table II. Table II

Many of these factors involve the practical aspects of residual stress analysis: correct preparation of the specimen surface (if possible)*, proper selection of radiation and filters, accurate alignment, corrections for beam penetration and high stress gradients. Others involve factors affecting any x-ray diffraction technique such as grain size, stacking faults, twinning and texture. An excellent handbook (Hilley et al., 1971) is available describing the procedures to control these factors. Some are dependent on the capability of the experimenter (alignment, sample position) or on electronic stability of the equipment and cannot be readily treated mathematically.

There are, however, biasing factors for which corrections are known.

1. Angular Dependent Intensity Factors

The Lorentz factor and polarization factors, both arising from the geometry of the diffraction process (Cohen, 1966; Cooper and Glasspool, 1976), and an absorption factor, resulting from differing path lengths in the specimen of incident and scattered beams when it is tilted by ψ (Koistinen and Marburger , 1959), are commonly combined into one term (LPA) given for the omega diffractometer and filtered radiation by:

*It is worth mentioning that the x-ray technique can be employed even when there are thin oxide or paint layers; the beam will readily penetrate such films. Wire brushing to remove such effects can produce severe stresses and is to be avoided.

$$LPA = \left(\frac{1 + \cos^2 2\theta}{\sin^2 \theta}\right)(1 - \tan\psi\cot\theta). \qquad (22)$$

The measured intensity at each angle need only be divided by Eq. (22) prior to processing.

The intensity across a peak is also dependent on the atomic scattering factor (International Tables for X-ray Crystallography, 1968) and the Debye temperature factor (which accounts for the reduction in intensity due to thermal motion) and strictly speaking these should be taken into account. For alloys, these two terms often become complex and are usually neglected. However with automated processing it is little effort to incorporate them.

Over the range of $154^\circ 2\theta$ to $158^\circ 2\theta$ where the most commonly used diffraction line for stress analysis of steel occurs with CrK_α radiation, Short and Kelly (1973) have calculated the change in the intensity factors. Table III Their values are summarized in Table III and show that the temperature factor is a very small correction in relation to the others, but the variation in the atomic scattering factor is significant. Tabulation of these factors applying to all radiations and materials are available, for example, (Evans and Littman, 1977; Hilley et al., 1971; Short and Kelly, 1973; the International Tables for Crystallography).

2. Beam Optics

The Ω and ψ diffractometers both employ a divergent primary beam and hence illuminate a considerable area of the specimen to provide good averaging over many grains, and both employ focusing of the diffracted beam. The angle between primary and diffracted rays depends on the horizontal and vertical divergence of the beam and on sample position.

a. Horizontal Beam Divergence

In the parafocusing method, true focusing demands that the sample surface lie on the focusing circle which is given by (Hilley et al., 1971):

$$R_{FC} = R_{GC}/2 \sin(\theta + \psi) . \quad (23)$$

This focusing actually requires a continuous change in the curvature of the specimen during θ and ψ tilts. Since this is generally not practical, an error will arise, which is dependent on the curvature of the sample and the horizontal beam divergence. The focus is an area, shown in Fig. 11. Marion (1972) has derived a simple formula to estimate the error in the peak shift between two ψ values due to beam divergence. Defining α as half the angular beam divergence, the peak shift in degrees 2θ, $\delta(\Delta 2\theta_{BD})$, between the $\psi = 0^{\circ}$ and $\psi = \psi^{\circ}$ inclination, is:

Fig. 11

$$\delta(\Delta 2\theta_{BD}) = (\Delta 2\theta)_{\psi=0} - (\Delta 2\theta)_{\psi=\psi}, \quad (24)$$

where $\Delta 2\theta_{\psi} = \frac{180}{\pi} \cdot \frac{R_{GC}}{R_p'} \cdot \frac{\tan\alpha}{2} \left[\frac{\cos(-\alpha+\psi+\varphi)}{\cos(-\alpha+\psi-\varphi)} - \frac{\cos(\alpha+\psi+\varphi)}{\cos(\alpha+\psi-\varphi)}\right]$, and $\varphi = 90 - \theta$.

The term R_p' is given in Eq. (17).

Because there is a distribution of intensity between the central beam and the left and right portions, the actual peak shift will be less than $\delta(\Delta 2\theta)_{BD}$. It has been shown (Zantopulos and Jatczak, 1970) that the centroid of the diffracted beam approached a limit of 1/3 of the $\delta(\Delta 2\theta)_{BD}$ value. Therefore, as a conservative estimate one can use 1/2 of the value calculated in Eq. (24). An estimate of the typical magnitude of this quantity is given in Table IV. It was also found that the stationary slit method yields $\approx$ 1/3 the error as in parafocusing in the range of 2θ appropriate for stress measurements of steel with CrK_{α} radiation ($2\theta = 156^{\circ}$).

Table IV

This is another factor favoring the stationary slit method.

b. Vertical Beam Divergence

Grains that have planes slightly tilted from that of the diffracting position for a parallel incident beam may contribute weakly to a peak, and give rise to an apparent peak shift (Hilley et al., 1971). The shift depends on the amount of texture and the slit system and is difficult to determine exactly, but is small if Soller slits are employed. An estimate is also given in Table IV.

* * * * * * * * * *

A defocusing error exists when using a position sensitive detector in parafocussing geometry. The PSD, effectively a long, straight wire, is only tangent to the focusing circle over a small range. That portion which is not tangent causes a subsequent defocusing error which has been treated analytically (James and Cohen, 1979) and is fortunately negligible for the usual diffractometer radii. It should also be pointed out that there is a paralex error with this device; if the beam is incident at 85° instead of 90°, resolution decreases $\approx$ 30 pct. For the region near the top of even a broad peak there should be little effect due to this phenomenon, but this needs to be examined experimentally.

c Alignment Error

Two sources of error are dependent on the alignment: sample displacement and missetting of the ψ axis. The magnitude of the error due to sample displacement is dependent on the type of focussing as discussed in Sec. III. B. 3; it is approximately five times greater in parafocusing geometry than in stationary slit geometry. A similar error is produced by a missetting of the ψ axis as shown in Fig. 12 for the Ω diffractometer. The axis of inclination of the sample, ψ, must be coincident with the 2θ axis or a peak shift will result. Marion (1972) has also examined this error and calculated the peak shift in degrees 2θ to be:

Fig. 12

$$\delta(2\theta)_{\psi A} \simeq \frac{-360}{\pi} \Delta X' \frac{\sin\theta \cos\theta \ (1-\cos\psi)}{R_p \sin \ (\theta+\psi)} , \qquad (25)$$

where $\Delta X'$ is the effective displacement. This source of error can be important on diffractometers employing an attachment to give the ψ rotation. In the side-inclination technique the same type of error arises if the incident beam is not symmetric about the ψ axis.

Typical errors for these effects are included in Table IV.

With parallel beam geometry, these errors do not occur (James and Cohen, 1977; Chrenko, 1977; and Aoyama et al., 1968). Also, the shape of the specimen is less important with this technique because there are no errors due to horizontal beam divergence. When used in conjunction with a normal x-ray tube, however, the measured intensity is reduced over that obtained in focusing geometries due to instrumental broadening, and this causes the precision in locating a position on the diffraction line to decrease (James, 1977). This does not seem to be the case however when specially designed x-ray tubes are employed (Klug and Alexander, 1974; Chrenko, 1977).

3. Beam Penetration

When a steep stress gradient exists in the surface layers of a sample, the measured diffraction angles for different ψ values will represent a sampling of a different mean stress because of a change in the depth of beam penetration. As an example, when using CoK_α in iron, 50 percent of the diffracted radiation penetrates to a depth of 7.3 μm at $\psi = 0$. At $\psi = 50^\circ$, the penetration depth is only 4.5 μm.

Correction procedures involve determining the stress gradient by electrochemically removing thin surface layers. Derivation of proper

correction formula and procedures to use them are adequately described by Hilley et al. (1971) and Lei and Scardina (1976). Corrections for stress relaxation due to layer removal are also presented by both authors.

Fig. 13 Fig. 13 illustrates the effect of the different correction factors on a stress profile produced by light peening. Curve 2, obtained after accounting for beam penetration, demonstrates the considerable change in observed surface stress due to this factor. Relaxation after layer removal, represented by curve 3, is seen to become significant as greater depths are removed.

C. Precision of the X-ray Stress Measurement

1. Introduction

The angle of the diffraction peak (in any ψ position) may be determined from any consistent feature of the line profile. While graphical methods can be used, the need to correct data for the angular dependnet factors (Sec. IV. B. 1.) has promoted the use of curve fitting procedures. In the United States, the traditional method has been a fit of a parabola to three points near the peak maximum (Koistinen and Marburger, 1959). But with the increased use of computerized instruments or a position sensitive detector, improved precision can be obtained with more sophisticated curve fitting techniques involving many points (James and Cohen, 1977). Three such procedures will be compared and then the effect of counting statistics will be discussed.

2. Methods of location of the Diffraction Peak

The centroid of a diffraction peak has been used in x-ray stress measurements (Ladell et al., 1959; Pike and Wilson, 1959; Singh and Balasingh, 1971; Baucum and Ammons, 1973). In Japan, the half-value breadth and quarter-value breadth (The Society for Materials Science, Japan, 1973) have been adopted. These involve using the midpoint of a chord drawn through the profile at the indicated height. The peak of the diffraction profile may also be represented by the maximum in a least squares fit of a parabola to all the data points in the top $\approx$ 15 pct of the profile (James and Cohen, 1977; Kirk, 1971). For European practice See Faninger and Wolfstieg (1976).

The peak-to-background ratio is usually poor in residual stress measurements, especially with hardened steels. When employing the centroid or half-value breadth, background is subtracted, and this introduces an additional error. For the least-squares parabola, the entire profile need not be used. The background must be subtracted only when determining the region of curve fitting (James and Cohen, 1977). Because the least-squares parabola gives equal weight to all observed data points background subtraction does not affect the maximum (as long as the region is a good approximation to a parabola).

These three methods are compared in Table V (from James, 1977); the least squares parabola provides a considerable improvement in precision over the other methods for the 1045 steel with a broad profile and low peak to background ratio.

Table V

A problem which is usually ignored in stress measurement by x-ray diffraction concerns the asymmetry caused by the K_{α_1}-K_{α_2} doublet. The overlapping

profiles with their different intensities can lead to systematic errors in the line positions as the weight of the K_{α_2} peak changes due to increased smearing at different ψ inclinations. Often, large receiving slits are used (Hilley et al., 1971) which broadens the distribution at all ψ tilts. Macherauch and Wolfstieg (1977) describe the use of special detector slits in which a symmetrical intensity distribution is achieved.

3. Errors Due to Counting Statistics

Treatments of counting statistics for the different numerical methods for determining line-profiles can be found in the literature (Wilson, 1967; Thomsen and Yap, 1968).

For residual stress measurements and parabolic curve fitting, available procedures range from comprehensive analytical expressions using a least - squares fit of many points and applicable to both the $\sin^2\psi$ and two-tilt techniques (James and Cohen, 1977), to simple approximations applied to the two-tilt/three-point parabola curve fitting method (Kelly and Short, 1970). The former is applicable to computerized data collection techniques while the latter is excellent for manual measurements. Both procedures may be used for predicting the time of data collection for a given statistical error; in fact, the latter procedure is conveniently displayed in graphical form (Hilley et al., 1971).

The precision may be improved by simply increasing the accumulated counts at each data point. Increasing the size of the angular increment between data points which are in the upper 15 pct of the peak intensity will also improve the standard deviation for the three point parabola. James and Cohen (1977) have demonstrated that when automated data collection is used, the use of multiple data points (rather than three) and a least-squares parabolic

fit significantly improves the observed reproducibility. They have also shown that the $\sin^2\psi$ technique can be carried out to the same precision as the two-tilt technique, again in the same total time.

D. Summary

It is instructive to consider the total error possible in a residual stress measurement due to all the factors listed in Table II. While Table IV is useful in estimating the typical instrumental errors, samples circulated to many investigators can give an unbiased view of the combined accuracy and precision to be expected. The following data is taken from Hilley et al., (1971) and should be compared to Table IV.

1. SAE Round Robin No. 3. (11 laboratories reported, 1959)
   a. flat specimen (broad peak)
      stress level: 14 MPa
      standard deviation among laboratories: $\pm$ 10.3 MPa
   b. 1010 annealed flat steel (sharp peak)
      stress level: -5 MPa
      standard deviation: $\pm$ 16.5 MPa
2. SAE Round Robin No. 4 (25 laboratories, including many with little or no experience in residual stress measurements)
   a. flat, shot-peened (R_c 63)
      stress level: 593 MPa
      standard deviation: $\pm$ 41 MPa
   b. 1045 Round bar, 6.22 cm diameter (R_c 61/62)
      stress level: 910 MPa
      standard deviation (axial direction): $\pm$ 56.5 MPa
      standard deviation (longitudinal direction): $\pm$ 72 MPa

V. FUNDAMENTAL PROBLEMS

A. Introduction

The lattice strain deduced from changes in position of an x-ray diffraction peak represents an average value in a given direction only for those grains in the polycrystalline aggregate which are oriented to diffract and the average is over the coherently diffracting regions, subgrains, regions between dislocations, etc. Furthermore, in elastically anisotropic materials, the conversion of strains into stresses implies that the residual stress system is essentially uniform in all grains irradiated in a single phase material or constant throughout one phase in a two phase material. There may be wide variations if a region has undergone appreciable plastic deformation (and this variation could be quite important). Thus, while the residual lattice strains (RLS) may be measured without ambiguity, some care is needed in relating these to an equivalent stress system.

Problems that arise due to these phenomena (and some of the opportunities for interesting studies that result from them) are considered in this chapter.

B. Elastic Anisotropy

The various formulae used to convert the RLS to residual stress, as given in Eqs. (1) - (12) were derived from the theory of isotropic elasticity in which bulk elastic constants are valid. These bulk elastic constants are usually measured by mechanical methods. Unfortunately, polycrystalline materials are usually not elastically isotropic and the selective nature of x-ray diffraction amplifies this difference. In order to account for this, appropriate x-ray elastic constants are often employed. These can be determined either theoretically or experimentally.

The theoretical methods have been recently reviewed by Macherauch and Wolfstieg (1977). The elastic behavior of a polycrystalline aggregate can be calculated from that for a single crystal. Some assumption must be made, however, the most common being that of Voigt, who assumes equal strainsin all directions, Ruess, who assumes equal stresses in all crystallites and a modification of Kröner's "coupled crystallites" model (which involves the coupling of an anisotropic crystal with an isotropic matrix). The estimates based on Kröner's theory appear to coincide best with experimental evidence (Macherauch and Wolfstieg, 1977). X-ray elastic constants have also been calculated by using one or more of the above assumptions and considering the effects of preferred orientation (Taira and Hayashi, 1970; Evenschor and Hauk, 1975a) and the effects of more than one phase (Arima et al., 1971; Evenschor and Hauk, 1975a,c; Hauk and Kockelmann, 1977). The applicability of these assumptions to different materials systems and deformation has been reviewed by Dölle and Hauk (1977).

Measured x-ray elastic constants depend on lattice-plane (Dölle and Hauk, 1979), second phase components (Macherauch,1966; Prümmer and Macherauch, 1966), grain size, and microstructure (Faninger, 1970), heat treatment (Prümmer, 1970) and deformation (Prümmer and Macherauch, 1965; Esquivel, 1969; Taira et al., 1969; Rutledge and Taylor, 1972; Marion and Cohen, 1977). The magnitude of the effect depends on the hkℓ reflection, but differences of 25% or 40% between theoretical and experimental values are often quoted (Marion and Cohen, 1977). These variations are not yet fully explained by the existing theories and demonstrate the need (if at all possible) for measuring the x-ray elastic constants for a specimen exactly the same (in terms of composition, grain size, heat treatment and deformation history) as the materials being studied. The experimental technique for this involves elastically deforming a specimen on the diffractometer to known stresses, while measuring the peak shift (Barrett and

Massalski, 1966; Klug and Alexander, 1974; Society of Materials Science, Japan, 1974; Cullity, 1977). Prevey (1977) describes in detail an apparatus and procedure for determing $E/(1+\nu)$ in four point bending and includes a good compilation of x-ray elastic constants for iron, nickel , copper aluminum and titanium alloys (see also Macherauch,1966; Ranganathan et al., 1976).

While this problem is important when absolute values of residual stress are desired, if only relative values are needed, such as in quality control, or in determining the effects of processing, the x-ray elastic constants determined from theoretical calculations or from prior measurements in the literature are sufficient.

C. Plastic Deformation

1. Background

Plastic deformation produces a complex distribution of heterogeneous internal strains Factors may contribute to a peak shift which are microscopic in nature. The shift is termed "anomalous" because mechanical methods of residual stress measurement sometimes do not indicate such effects. Indeed, this is to be expected since the cause is on a scale smaller than that resolved by mechanical techniques! Such microstresses may be of considerable importance in understanding material behavior and describing the effects as "anomalous" is unfortunate. There are really basically three recognizable "anomalies". First, RLS are developed during uniaxial plastic deformation (UPD) which contribute to the stress measured by x rays but are not found with mechanical techniques. Second, even when elastic anisotropy is taken into account, the measured surface residual stress may depend on the particular diffraction plane utilized. Third, oscillations and/or curvatures in d vs. $\sin^2\psi$ sometimes occur rather than the linearity predicted by Eq. (3).

2. Uniaxial Plastic Deformation

When a metal is plastically extended and then unloaded, dissection (mechanical relaxation) does not reveal a stress whereas the x-ray method does. While most practical methods of residual stress inducement are not characterized by unidirectional loading, this discrepancy is useful in demonstrating the relationship between macrostresses and microstresses. Four recent review articles (Faninger, 1970; Dölle et al., 1976a ; Cullity, 1977 ; and Macherauch and Wolfstieg, 1977) have adequately reviewed the literature and only a summary is presented here:

1) The surface residual stress is compressive after tensile-deformation and increases with increasing plastic strain. These surface stresses have been found in both single phase and multiple-phase alloys.

2) In single phase alloys the residual stress is found to decline towards the interior of the sample and exhibits macroscopic equilibrium over the cross section.

3) In two phase materials such as steel and age-hardened aluminum alloys the magnitude of the observed residual stress does not exhibit macroscopic equilibrium over the cross section - e.g. the stress is detected essentially unchanged, through the thickness.

The cause of the surface residual stress is most likely due to the difference in hardening of surface layers and the interior, and that grains in the surface are less restrained during plastic flow than those in the interior and thus have a lower yield stress (see Garrod and Hawkes (1962) for a classification of these and other contributory causes). These differences arise in both homogeneous and heterogeneous materials and can be expected to increase with increasing deformation, particularly the first cause. Both produce what are considered to be macrostresses.

The nonequilibrium of stresses over the cross section in heterogeneous materials is attributed to microstresses of the second kind. These appear to be out of balance because only one component is usually sampled by the x-ray technique. For example, the measured value may be the compensation of compressive residual stresses in a crystallite by tensile stresses in areas of high dislocation density. The latter areas do not contribute appreciabl to the peak of the diffraction profile whereas the "coherent" compressive region does. The sites of high dislocation density may be grain and subgrain boundaries, phase boundaries or other obstacles to dislocation motion such as inclusions and precipitates. In addition to this subtle coherency effect is the obvious case where the stress in one phase may compensate that in another, and only one phase is examined. A good example of this has been reported by Taira et al., (1974) in plain carbon steel. The magnitude of the microstresses increased linearly with carbon content up to .5% C enabling this component to be separated.

The microstresses which occur in heterogeneous materials after uniaxial plastic deformation contribute to the linear d-$\sin^2\psi$ relation and cannot be resolved from the macrostress. While qualitative interpretations of the microstresses are satisfactory, quantitative separation into the contributory causes requires much further work (Macherauch and Wolfstieg, 1977). However, for mechanisms involving local failure, it is the total which is probably important, not one or the other; the separation may not be worthwhile.

3. Diffraction Plane Dependence of the Measured Stress

Another result of UPD of iron is that measurements with the 211 diffraction peak give a smaller value of residual stress than is measured with

the 310 peak. This diffraction plane dependence occurs even when experimentally measured elastic constants are used for each peak indicating that the hkℓ dependence is not due to elastic anisotropy.

Table VI An example of such results for a steel is given in Table VI.

It has been suggested that this effect may arise from changes in beam penetration associated with the different radiations and diffraction angles (Doig and Flewitt, 1977a,b) but Dölle and Hauk (1977) have noted that the hkℓ dependence arises under conditions of texture development during plastic deformation, both in tensile and rolling deformation. Although further work is needed, this suggests that plastic anisotropy might account for this dependence. The (211) plane is a slip plane in b.c.c. structures whereas the (310) plane is not. In simple terms, for a macroscopic stress state a larger portion of the load will be supported by the stronger direction than the weaker ones, in agreement with Table VI. It would be interesting in this regard to examine the difference after removing surface layers, to see if in fact this is a phenomenon due to stress gradients.

A number of theoretical investigations have been undertaken to account for this hkℓ dependence of the measured stress in terms of elastic (Prümmer, 1967; Hosokawa and Nobunga, 1969; and Hosokawa et al., 1972) and plastic (Smith and Wood, 1944 and Hosokawa et al., 1972) anisotropy. Perhaps the most successful investigation is that of Taira and Hayashi (1971) who applied a theory of plastic deformation introduced by Oyane and Kojima (1955) to calculate the reorientation of crystallites based on operative slip systems in UPD. With an equation based on elastic cubic anisotropy (see Hosokawa et al., 1972, and Möller and Martin, 1939, for derivations of such formulae)

the relationship between the preferred orientation developed in UPD, the elastic anisotropy of the constituent crystals and the selective nature of the x-ray diffraction method were taken into consideration. The results demonstrated the sense and to some degree the magnitude of the lattice plane dependence of the measured residual stress.

The problem becomes more complicated in other plastic deformation processes such as rolling; plastic deformation theories have not yet been developed in this case which yield the relationship between the stress tensor and the crystallite orientation (Hosokawa et al., 1972).

4. Non-linearity of Lattice Spacing vs. $\sin^2\psi$

The problems discussed in Sec. V. C. 2. and V. C. 3. are fundamental in that the effects have a close relation to anisotropic deformation, texture development and microstrains; the x-ray method in fact is a useful experimental technique to investigate such problems. Practically speaking, however, there are few circumstances where problems actually arise due to these effects.

A more important phenomenon is the development of non-linear relationships between the lattice spacing and $\sin^2\psi$. Following Dölle and Hauk (1977) the types of non-linear behavior can be categorized according to the effects causing them.

Four types of possible lattice strain distributions (as a function of $\sin^2\psi$) are illustrated in Fig. 14. The linear relation, Fig. 14a, represents

Fig. 14

the case predicted by the classical x-ray stress analysis, Eq. (3), and is obeyed in the predominant number of experimental situations. The resulting stress can be macroscopic, or after uniaxial plastic deformation of heterogeneous materials, may be formed as a result of microstrain distributions (see Sec. V. C. 2.).

Fig. 14b. results when a strong stress gradient leads to changes in the lattice distortion over a distance less than the penetration resolution of the x-ray stress measurement (Shiraiwa and Sakamoto, 1972). It is assumed that no maxima or minima occur near the surface. In this case, the penetration depth of the x-rays varies with ψ so that each measurement at a different ψ inclination samples a different mean stress. Non-linearity caused by steep gradients can be investigated by etching off very thin surface layers, and looking for any marked changes, or non-destructively, be examining $+\psi$ and $-\psi$ tilts; the results should be the same if gradients are the cause (see below).

While such a factor can readily be seen to cause a systematic error as in Fig. 14b, Pieter and Lode (1976) and Doig and Flewitt (1977a, b) suggest that oscillations in "d" vs. $\sin^2\psi$ can occur if the stress gradient changes sign within the penetration depth, leading to a distribution as shown in Fig. 14c. There is no data to support this contention, and oscillations in d vs. $\sin^2\psi$ occur most often and most dramatically in homogeneous materials under deformation conditions that produce texture, such as rolling (Shiraiwa and Sakamoto, 1970; Marion and Cohen, 1974; Quesnel et al., 1978; Faninger, 1970). Steep stress gradients are not found in such cases, as evidenced by the difference in oscillations occurring with different radiations (Shiraiwa and Sakamoto, 1971 and Faninger, 1970). Furthermore, the oscillations persist even after the near-surface layers are removed (Quesnel et al., 1978).

While it is generally agreed that oscillations in d vs $\sin^2\psi$ are caused by strong texture development, a generally accepted method to account for the texture has not yet been agreed upon. Two major interpretations may be found in the literature.

The first relies on the selective nature of x-ray diffraction. Since only crystals with normals having a certain angular range about the incident

beam (associated with beam divergence, wavelength spread, and the range of diffraction angles) contribute to a reflection, a calculation of the effect is associated with averaging over ψ in accordance with the crystallite orientations. The effective x-ray elastic constants of each ψ can then be weighted using the preferred orientation and the models of Voight, Ruess or Kröner to obtain corresponding polycrystalline elastic constants from single crystal data (Shiraiwa and Sakamoto, 1970; Taira and Hayashi, 1970; and Faninger, 1970). Unfortunately, this method cannot be used in practice because of the long time required to obtain a pole figure as well as a stress. Furthermore, the calculated oscillations do not always agree in sign or magnitude with those observed; perhaps because of the ideal textures and/or shapes of maxima in pole figures that are employed in the calculations.

This problem can be circumvented by using "texture independent" ψ tilts (Hauk et al., 1975; Hauk and Sesemann, 1967; Dölle et al., 1977) for determining uniaxial stress. These are determined by the intersection of the theoretical curves of d vs. $\sin^2\psi$ based on the Ruess approximation and that of the single crystal equation* of Moller and Martin (1939). Solution to the latter demands some known relation between the stress tensor, σ_{ij}, and the orientation of crystallites (Hosokawa et al., 1972). These authors represent the texture in terms of ideal states which, especially in f.c.c. materials, are never fully achieved. The method recommended by the authors Dölle et al., 1977, involves the Ruess approximation of constant stress in all directions which is well known to be incorrect and applies only to uniaxial loading. Hence the procedures cannot be readily applied to determine the macro-residual stresses

*This single crystal elastic equation of Möller is identical to that discussed in Sec. V.C.3.

in most practical situations. Other methods are currently being tested by Dölle, Hauk and co-workers (Dölle and Hauk,1978).

The second interpretation attributes the oscillating dependence of d on $\sin^2\psi$ to the relief of microstrains during plastic deformation which is related to texture development. Originally proposed by Weidemann (1966) and Bollenrath et al., 1967, Marion (1972) and Marion and Cohen (1974) incorporated the predicted non-linear dependence into a general formula of residual stress analysis by x-ray diffraction. Because of its simplicity and direct applicability, the method is briefly reviewed here.

In this approach, the non-linear dependence of d on $\sin^2\psi$ is thought to be due to the relief of microstrains in subgrain interiors, which were oriented to be relieved by a dynamic recovery process (Bollenrath, et al., 1967; Weidemann, 1966). This produces a non-random distribution in the interplanar spacing which is related to any texture developed during the plastic deformation process. Marion and Cohen (1974) developed a distribution function, $f(\psi)$, describing the variation in interplanar spacing at each ψ inclination. By measuring both the interplanar spacing, $d_{\varphi,\psi}$, and the distribution function, $f(\psi)$, as a function of $\sin^2\psi$ for at least six ψ tilts, the non-linear dependence of d may be separated from the linear component through the following formula:

$$d_{\varphi,\psi} = (d_{max} - d_{\beta})f(\psi) + d_o(\frac{1+\nu}{E})\sigma_{\varphi}\sin^2\psi + d_{\beta}. \qquad (26)$$

The term d_{max} corresponds to the lattice spacing in a region that is fully relieved and d_{β} the lattice spacing in a region that has not been relieved.

The term $d_{max}-d_{\beta}$ thus represents the range of d spacings present. Actually the same range of d spacing could also be due to elastic anisotropy and the influence of neighboring grains, so the treatment is really more general than was originally proposed. (But there is no agreement between the stresses determined by this method and that from the "texture independent" ψ tilts that were discussed above, based on elastic anisotropy and the Ruess assumption). The distribution function describes the variation of d with orientation and is obtained by measuring the texture only in the region of the pole figure for which the residual lattice strain is measured. This is readily accomplished by simply measuring the peak height minus background or net integrated intensity of the diffraction peak of interest at each ψ inclination and along with the peak position, and normalizing the distribution function by setting $f(\psi) = 1$ at the maximum of the curve of integrated intensity. The correlation between the change in the distribution function and oscillations in d vs. $\sin^2\psi$ is shown vividly in Fig. 15. [When texture and oscillations are present it is important in measurements with the parafocusing method that a vertical slit be placed near the detector and only the horizontal receiving slit be moved. In this way at all ψ tilts the same portion of the diffracting cone is being sampled at all times. When texture is present the distribution of intensity around the cone is non-uniform.]

Fig. 15

Moderate rolling or uniaxial deformation does not usually cause texture in materials with an appreciable quantity of well distributed second phase. Thus this problem does not arise in steels with more than 0.4 wt pct carbon. One way to sort out these different interpretations would be to deform Al or W (being careful to minimize recovery) to produce a severe texture. If the effects that are observed in other materials are indeed due to elastic anisotropy, they should be minimal with these materials.

The final variation of d vs $\sin^2\psi$ to be considered is that in Fig. 14d. This unexpected effect is found after unidirectional grinding or milling, or on the surface of wheels upon measuring lattice strain distributions in both the positive

and negative ψ directions, or, alternatively, by measuring in the $\varphi = 0^{\circ}$ and $\varphi = 180^{\circ}$ directions (see for example, Krause and Jüle (1976)). The plain surface stress state ($\sigma_{13} = \sigma_{23} = 0 = \sigma_{33}$) assumed in the classical x-ray stress formula would predict identical overlapping lines, Eq. 13. Instead, there are curves which are split into branches after certain types of plastic deformation (Christ and Krause, 1975). This arises from the existence of large shear components (Evanschor and Hauk, 1975b) which can only occur if the x-ray beam is seeing the entire stress system, not just the surface. The various stresses and strains can be determined by the methods described in Sec. III.A.4. The fact that this effect is only detected in certain situations is puzzling, and further work in this area will be of considerable interest.

D. Summary

When making stress measurements with x-rays, it is necessary to keep in mind that when strong texture is produced during processing along with stresses, the d spacing may not be linear with $\sin^2\psi$. It is then important to use at least six ψ tilts in a measurement at both $+\psi$, and $-\psi$. The Marion-Cohen method appears to be a practical procedure for separating the macrostress and the range of d spacings present due to microstresses, whether these are due to stress relief or anisotropy. The range of d spacings may be particularly interesting in studying failure mechanisms, although this has not yet been attempted. The exact cause of the oscillations and the variation of stress with reflecting plane certainly needs additional study.

The stresses measured with x-rays include both macrostresses and microstresses (those averaged only over the size of the coherent reflecting regions, that is, the spacing between dislocations, or with subgrains). Thus when the entire material is subjected to extensive plastic deformation, the x-ray method may yield results different from those obtained by mechanical means,

because the x-ray method averages over a smaller gage length and also because x-rays have a low penetration depth. The method is a particularly interesting tool for studying stress vs depth and it has the additional advantage that the stress in several phases can be examined simultaneously (see for example Hanabusa et al., 1969).

VI. APPLICATIONS

A. Introduction

With the nondestructive x-ray method it is possible to study the stress distribution, which results from a manufacturing operation, and its effect on service of the part. Stresses can arise in heat treating, carburizing and electroplating, or machining, forming,and shotpeening. The resultant stresses can be important in determining the behavior of the material - its stress corrosion, dimensional stability, and behavior under dynamic loads such as fatigue (in which case the surface or near surface stress is particularly important). Of course residual stresses are just one among many important aspects of a surface, along with its composition, structure, topography, morphology, and distribution of second phases, hardness and work hardening characteristics.

We first review the literature on stresses produced during manufacturing and then the changes in stress distribution during dynamic loading. Our main goal is to provide the reader with a guide to recent literature on the application of stress measurements by x-rays to a variety of practical situations. An exhaustic literature listing is also available by J. Hauk (1976) in Hartrei- Techn. Mitt. 31, pp. 112-124.

B. Production and Effects of Residual Stresses

1. Heat Treatment

During heating or cooling, stresses may arise due to differences in the rate of temperature change between the surface and interior, or from differences in the coefficient of expansion of the different phases present.

The local yield strength may be exceeded at some temperature, resulting in non-uniform plastic flow, and large stresses may occur. Specific examples of such stress distributions can be found in Barker and Sutton, (1967) for an Al alloy, and in Volorinta, (1965) for a low carbon steel.

In materials that undergo phase changes even more complex stress states may develop. For example in hardenable steels, martensite may form first at the surface (on cooling) causing plastic extension of the center. When this phase subsequently forms in the center of the piece, the surface is put in tension. Valorinta (1965) discusses this problem and offers some solutions; see also Snyder (1952), Nakagawa et al., (1972), and Nakagawa et al., (1974). Tempering, aging and reversion can alter the stress pattern (Liss et al., 1966; Evans, 1969; Hanke, 1969; Nelson et al., 1969; Nelson et al., 1970).

A typical stress pattern in a quenched plain carbon steel due to thermal

Fig. 16 stresses is shown in Fig. 16.

As pointed out earlier, the stresses in each phase can be examined with x-rays. An interesting example associated with heat treatment can be found in the study of stresses in the ferrite and austenite phases of a stainless steel (Takada and Matsumoto, 1976).

2. Mechanical Working of Surface Layers

During shot peening, surface layers are extended. Due to the resistance of the interior to this extension, the surface is put into compression. This process is, therefore, particularly useful in reducing crack propagation rates. The

Fig. 17 stress gradient is sensitive to many variables. Fig. 17 shows that increasing

Fig. 18 shot size increases the depth of the compressive zone, while Fig. 18 reveals that increased hardness of the base alloy results in a higher peak stress.

Such variables and others have been studied extensively in steels (Lessells and Brodrick, 1956 and Robertson, 1969), aluminum alloys (Lei and Scardina, 1976), and Ti alloys (Singh et al., 1973). Because of the high gradients produced by shot peening profiles of stress vs. depth are generally of interest (Iwanaga et al., 1972).

An example of the value of knowing stress distributions is the study by Nelson et al. (1969, 1970). In a shot peened SAE 1045 steel subjected to non-rotating alternating bending stress, cracks propagated in from the surface, but stopped or slowed where the compressive stress was largest below the surface.

The effect of prolonged exposure of shot peened steels (Diesner, 1969) and Ti alloys (Braski and Royster, 1967) to rolling stresses and moderate temperatures such as in lubricants has been studied.

Dietrich and Potter (1977) studied the stresses around fastener holes ; see Fig. 19. This study is a particular example of the need for such measurements, as the compressive zone is wider and the stress larger than predicted by theory. See also Flemmer and Chandler (1976).

Fig. 19

The effect of stresses from mechanical surface treatment on fatigue behavior of steel has been examined (Hayashi et al., 1973; Ivanov and Pavlov, 1976 ; Turovskii et al., 1976). A particularly interesting (but often overlooked)study is that by Evans, Ricklefs and Millan (1966). They produced surface compressive stresses by shot peening in hard and soft steels and examined both the stresses, and the surface cold work(by Fourier analyzing peak shapes to measure microstrain distributions and subgrain size). The effects of the cold work and stresses on fatigue were separated by carrying out fatigue tests with and without superimposing mean stresses

to cancel the residual macrostresses. In soft steels, cold work is more important in enhancing the fatigue limit than the stress, whereas the reverse is true for hard steels.

3. Machining

The combined rapid heating and surface extension in this process produces surface residual stresses, the final distribution being strongly dependent on the exact details of the machining operation, cutting speed, depth, lubricat .., type and sharpness of the cutting tool. Henriksen, (1957) summarizes the (extensive) work prior to 1957 with ceramic and carbide tools. The resultant stresses can affect dimensional stability (Marschall and Maringer, 1977).

Koster et al., (1970) made an extensive study of surface integrity in machining steels and Ti alloys, including the effects of induced phase transformations. It is interesting to note that phase transformations did not occur in milling operations, and hence similar stress patterns were found in both alloys. Grinding has been examined by Singh et al.,(1973).

Mechanical and x-ray methods for determining stresses in machining have been found to agree in a high strength aluminum alloy (Senatorova and Samoilov, 1969). Prevey (1976) found that grinding and turning steels and Al alloys does not cause sufficient texture development to produce non-linearities in d vs $\sin^2\psi$ (see also Iwanaga et al., 1972). But results in this area need to be considered with caution in view of the ψ splitting discussed in Sec. V.C.4. and the fact that stresses which are normal to the surface are measured.

With a small x-ray beam size (0.6 x 0.05 - 0.3 cm) Prevey and Field (1975) examined gently and abusively ground steels, inconel and an aluminum alloy; large variations in surface stress occurred across a specimen, and both tensile and compressive regions were visibly burned, which could lead to local phase transformation as well as oxidation.

Cracking in ground surfaces of carburized and hardened parts has been found to occur in regions of high residual tensile stress and lowered hardness, suggesting that tempering had occurred in such regions (Buenneke, 1969, Shiraiwa and Sakamoto, 1973).

The residual stresses in the individual phases in ground, or lapped WC-Co alloys have been studied (Hara et al., 1970; Spiriana et al., 1975). The differences in coefficient of expansion of the precipitates and the matrix, which produce the stresses, makes processing particularly critical, and hence the stress pattern is important.

The effect of machining stresses on behavior of steel in fatigue has also been investigated (Tarasov et al., 1957; Syren et al., 1976a and 1976b.) It is particularly interesting to note that a good correlation was obtained between fatigue limit and the peak stress below the surface, but not with the surface stress (Tarasov et al., 1957). In agreement with the findings by Evans et al., (1966) on the effect of shot peening, reported in the previous section, Syren et al., (1976a and 1976b) found that, for soft steels, surface hardening due to machining was more important in determining the fatigue limit than stresses, but the reverse was true for hard steels.

4. Carburizing, Nitriding, Surface Coatings

Koistinen (1958) measured residual stress distributions in case hardened steels with x-rays and related the stresses in the case to the sequence of phase transformations in the case and core associated with heat treatment. The case was found to be in compression, with the maximum stress at about halfway through the case. The stress became tensile at the case-core boundary. Other interesting studies in this area can be found in Koistenen and Marburger

(1959) and Motoyama and Horisawa, (1969); the effect of tempering after case hardening is examined in Kirk et al. (1966) and MacDonald (1970).

In case hardened steels containing Mn and Cr Ericsson and co-workers (1976 and 1978) have found that the alloying elements are oxidized, resulting in surface pearlite early during quenching and a resultant tensile stress. The addition of nitrogen suppresses the pearlite and the tensile stress. (At the University of Linköping, Sweden, Ericsson and his group are actively pursuing the analytical calculation of stress patterns after case hardening, taking into account the various transformations and their kinetics.)

In a study of induction hardening, Ishii et al., (1969) found that tensile stresses at the boundary of the hardened zone are more likely if the layer is thin; also, the stresses are greater after progressive quenching than after static quenching.

Protective surface layers for various environments can be produced for example by electroplating, spraying, flame deposition and explosive cladding. Electroplating often seems to produce residual tensile stresses which are sensitive to layer thickness only for small thicknesses (Hammond and Williams, 1960; Bush and Read, 1964; Revay, 1975) and are a function of the additive concentration in the plating solution (Hinton et al., 1963).

Stress patterns are found in other methods of depositing protective coatings. Kornev, et al., (1976) investigated both macro and micro stress levels in flame deposition. Deposition of powdered nickel and copper oxides was brought about by detonation of gaseous mixtures over a base of nickel or titanium. The surface layers are heated much more extensively than the substrate and during cooling, are prevented from contracting by the cool base metal. This places the surface in tension. The coating is built up in

layers; after some thickness the tensile macrostresses decrease and compressive stresses are found (when the thickness is greater than 250-275 μm). The inner layers adjoining the substrate are under tension as expected.

Explosively clad austenitic stainless steels have been studied by Oda and Miyagawa (1976). This process creates tensile residual stresses in the surface layer of the stainless steel, highly tensile stresses in the bonded zone, and compressive stresses in the mild steel base.

5. Other Investigations

The role and measurement of residual stress by x-ray diffraction is important in many areas not covered by the previous sections. Dimensional instability after fabrication and failure during service are, in part, related to residual stresses, and plague the welding engineer. In a recent review of techniques of stress measurement applicable to welding, Parlane (1977) lists seven references to recent applications of the x-ray technique of which Wohlfahrt (1976) is perhaps the most important. Digiacomo (1969) has recently discussed many of the problems in applying and interpreting the x-ray measurement under welding conditions and demonstrates a linear correlation between weld stability and residual stress in butt welded plates. [Taira and Matsuki (1968) suggest that by slightly oscillating both the specimen and x-ray film the precision of the x-ray measurement in the coarse grained heat affected zone can be improved by permitting a greater number of grains to be sampled.]

The role played by x-ray stress measurements in the wear of sliding materials has also been studied (Muro and Tokuda, 1968; Mura et al., 1973; Wheeler, 1974 ; Krause and Jühe ; 1977). Residual stress measurements reveal information about the contact stress developed in service.

The influence on wear of running conditions such as relative velocities, vibration, and temperature has been examined.

The x-ray technique has also been applied to the problem of stress corrosion cracking (Kawai and Takizawa, 1974; Cathcart, 1976; Cheng and Ellingson, 1976) and to the analysis of stresses in manufactured metal components (Nolke and Speicher, 1973; Goto, 1974; Larson, 1974; Wolt et al., 1977) and ceramics (Grossman and Fulrath; 1961).

C. Residual Stresses in Fatigue

It is generally accepted that fatigue strength is significantly increased by a compressive residual stress and lowered by a tensile residual stress (Dolan, 1959) at least in hard materials (see Sec. VI. B. 2). Evidence for this has been reviewed by Frost, Marsh and Pook (1974). The residual stress state significantly influences the propagation of micro and macro cracks and attempts have been made to account for both residual and mean stresses in fracture mechanics (Elber, 1974; Underwood, Pook and Sharples; 1977) and damage accumulation theories (Kempel, 1971; Landgraf, 1973). Macroscopic residual stresses are not expected to influence initiation of cracks since this is associated with localized surface regions of cyclic plastic strain attributable to alternating shear stresses. But the microstresses measured by x-rays could be important.

The effect of macro-residual stresses on fatigue is similar to a mean stress except that the former may relax while the latter is kept constant by an external load. Relaxation is therefore an important phenomenon in assessing the influence of residual stress. Rosenthal (1959) has collected data on residual stress relaxation from various sources and found that this occurs when the resulting value of the maximum resolved shear stress from both the applied and residual stresses exceeds the yield stress in shear of the

material.

Several investigators using the x-ray technique have shown relaxation occurring well below the endurance limit (Pattinson and Dugdale, 1962; Hayashi and Doi, 1971; Gould and Pittella, 1973). It has been suggested that stress concentrators may be the mechanism for relaxation in this regime (Nelson et al., 1970; Ericsson et al., 1971; Turovskii et al., 1976). Support for this idea of local yielding can also be found in the work of Morrow and Sinclair (1960) who found that the harder the steel, the less the fading. Perhaps another example of this effect is the recent finding that in steels containing appreciable quantities of pearlite, stresses are detected with x-rays when there were none initially (Morrow et al., 1960; Taira et al.,1969; Ziegeldorf, 1976) and that stresses can increase as well as decrease (Ericsson, private communication). There will always be some form of stress concentration, grain junctions, dislocation pile-ups, etc.

The majority of the investigations has been conducted at or above the endurance limit. The relaxation process may be divided into two regions (Kodama, 1971), the first occurring after gross yielding and the second occurring below the limit for this. The former involves macroscopic yielding of the surface such that a surface residual stress should, after unloading, be opposite in sign to the direction of loading (Kodama, 1971, 1972; Nago and Weiss, 1977; Quesnel et al., 1978). In measurements taken after each half cycle, Quesnel et al., found the residual stress was indeed dependent on the direction and magnitude of loading. This has also been found by Kodama, (1972)and Ziegeldorf, (1976). The manner of unloading also affects the stress (Ziegeldorf, 1976).

The second region involves microplastic behavior and a gradual reduction in residual stress with cycles is observed. The relaxation rate is most rapid

in the early part of fatigue life (Morrow et al., 1960; Koves, 1965; Esquivel, 1968; Ericsson et al., 1971; Seppi, 1976; and Leverant et al., 1978). Quantitative relations based on a linear proportionality between residual stress and the logarithm of the number of cycles have been empirically established (Kodama, 1971, 1972; Potter and coworkers, 1972; Wohlfahrt, 1973; Radhakrishnan and Prasad,1976). As an example, the latter authors proposed the following relation based on results with SAE 1008 steel:

$$\sigma_{R_\ell} = \sigma_{R_o} - \frac{RT}{\beta_\ell} \log (N+1) \qquad (27)$$

where σ_{R_ℓ} and σ_{R_o} are the instantaneous and initial value of the residual stress and β_ℓ is a constant. Increasing relaxation with higher temperature has been demonstrated by Potter and Millard (1977) in 7075-T6 aluminum alloy without cycling and by Leverant et al. (1978) in Ti-6Al-4V subjected to bending. It cannot be determined, however, if this data follows Eq. (27).

The constant β_ℓ depends on the material, cyclic stress amplitude and the stress distribution. To demonstrate the influence of the latter quantity Esquivel and Evans (1968) has shown that the degree of relaxation increases with increasing stress gradient in shot peened 4130 steel and both Esquivel and Evans (1968) and Hayashi and Doi (1971) have found that the greatest relaxation takes place on the surface.

Leverant et al. (1978) have shown that not only is the strain amplitude important, but also cycling about a mean strain significantly affects the relaxation. A mean strain of -.3 percent was found to induce greater relaxation in shot peened Ti-6Al-4V than a mean strain of +.3 percent. This was to be expected since a compressive surface stress was induced by shot

peening, and therefore the sum of residual and applied stresses was greatest with a compressive mean strain. The stresses in steel in different phases may depend on whether transformation occurs during the deformation (Beumelburg, 1974).

Although the validity of a general formulation such as Eq. (27) may be questioned, relaxation of surface residual stresses is known to occur at or near the fatigue limit. Well above this region, i.e. in the low cycle fatigue region, the residual stress state is dependent on the direction and magnitude of loading. Below the fatigue limit, relaxation may still take place, as there will always be stress concentrators, but definitive studies are lacking as yet. It is well to recognize, however, that the influence of compressive residual stresses in increasing fatigue life is highly dependent on their stability, since relaxation may take place early in the fatigue process.

D. Summary

The processing operations which produce residual stresses do so because of non-uniform plastic flow whether due to large temperature gradients, volume changes due to phase transitions, or from metal flow. The specific process has a large influence on both the magnitude of these residual stresses and their distribution in the depth, as does the material itself.

The presence of these residual stresses affects dimensional stability, the kinetics of stress corrosion cracking and the fatigue performance of a component. It is clear that cold working a surface layer has a larger influence on behavior than residual stresses for soft steels, but the reverse is true for hard steels.

It is difficult to draw firm conclusions on the effect of residual stresses on fatigue behavior perhaps because of altered physical or metallurgical properties during fatigue (e.g., hardness). However, the x-ray technique

is fundamental to such investigations because of its nondestructive nature. An accurate appraisal of the influence of stresses on fatigue must await better understanding of their stability. It is clear that especially in low cycle fatigue, or near stress concentrations, that stresses are altered quickly and considerably so that the initial stress cannot play an important role. Also results depend on whether the materials are released from tension or compression or whether the load is reduced slowly. It would be an important contribution to the currently increased interest in this area if more workers followed the stress pattern in their specimens as well as the other factors being studied.

VII. ACKNOWLEDGEMENTS

The authors would particularly like to thank ONR for their continued interest and support of research in this area. Dr. H. Dölle provided helpful comments on the final manuscript.

REFERENCES

Air Force Materials Laboratory (1976). Proc. of a Workshop on Nondestructive Evaluation of Residual Stress, Nondestructive Testing Information Analysis Center, Southwest Research Institute, 8500 Culebra Road, San Antonio, Texas 78284 (1975).

American Society for Testing Materials (1977). Standards, Part 10, p. 147.

Andrews, K. W., Gregory, J. C., and Brooksbank, D. (1974). Strain 10, 111-116.

Aoyama, S., Satta, K., and Tada, M. (1968). J. Society of Materials Science 17, 1071-1107.

Arima, J., Hosokawa, N., and Honda, K. (1971). Proc. of the Seminar, X-Ray Study on Strength and Deformation of Metals, Tokyo, Japan, 1-8.

Baldwin, W. M. (1949). ASTM Procs. 49, 539.

Barker, R. S., and Sutton, J. C. (1967). In "Aluminum" (K. R. Van Horn, ed.), Vol. III, Chap. 10. American Society for Metals, Metals Park, Ohio.

Barrett, C. S. (1977). Adv. in X-Ray Analysis 20, 329-336.

Barrett, C. S. and Massalski, T. B. (1966). In "Structure of Metals," 3rd edition, pp. 466-485. McGraw-Hill, New York.

Barrett, C. S., and Predecki, P. (1976). Pol. Sci. and Eng. 16, 602-608.

Baucum, W. E., and Ammons, A. M. (1973). Adv. in X-ray Analysis 17, 371-382.

Berg, H. M., and Hall, E. L. (1975). Adv. in X-ray Analysis 18, 454-465.

Beumelburg, W. (1974). (Dissertation), Univ. Karlsruhe.

Bollenrath, F., Hauk, V. and Müller, E. H. (1967a). Z. Metallkunde 58, 78-82.

Bollenrath, F., Hauk, V., and Weidemann, W. (1967 b). Archiv. für das Eisenhütt 38, 793-800.

Bolstad, D. A., and Quist, W. E. (1965). Adv. in X-Ray Analysis 8, 26-37.

Borkowski, C. J., and Kopp, M. K. (1968). Rev. of Sci. Inst. 39, 1515-1522.

Braski, D. N., and Royster, D. M. (1967). Adv. in X-Ray Analysis 10, 295-310.

Buck, O., and Thompson, R. B. (1977). Proc. of the ARPA/AFML Review of Progress in Quantitative NDE, Tech. Rpt. AFML-TR-77-44, 84-92.

Buenneke, R. W (1969). Society of Automotive Engineers, pamphlet 720243, SAE SP-362.

Bunce, J. (1977). Offshore Engineering, 43-44.

Bush, G. W. and Read, H. J. (1964). J. Electrochemical Society 3, 289-295.

Catalano, S. B. (1976). AD-A041147, National Technical Information Service, Springfield, VA., 22161

Cathcart, J. V. (1976). In "Properties of High Temperature Alloys, with Emphasis on Environmental Effects" , pp. 99-119.

Cheng, C. F., and Ellingson, W. A. (1976). In "Proc. of a Workshop on Nondestructive Evaluation of Residual Stress" NTIAC-76-2. Southwest Research Center, San Antonio, Texas, 89-100.

Chrenko, R. M. (1977). Adv. in X-Ray Analysis 20, 393-402.

Christ, E., and Krause, H. (1975). Z. Metallkunde 66, 615-618.

Cohen, J. B. (1964). Report on Tungsten Lattice Parameter Round Robin, X-Ray Subcommittee of SAE Iron and Steel Technical Committee, Div. 4.

Cohen, J. B. (1966), "Diffraction Methods in Materials Science." MacMillan Co., New York, p. 225.

Cole, H. (1970). J. Appl. Cryst. 3, 405-406.

Cooper, M. J., and Glasspool, A. V. (1976). J. Appl. Cryst. 9, 63-67.

Crisci, J. R. (1972). In "Periodic Inspection of Pressure Vessels", pp. 110-118. Inst. Mech. Eng., London.

Cullity, B. D. (1977). Adv. in X-Ray Analysis 20, 259-272.

Cullity, B. D. (1977). In "Elements of X-Ray Diffraction", pp. 447-477. Addison-Wesley, Massachusetts.

Denton, A. A. (1966). Metallurgical Reviews 11, Review 101. 1-22.

Denton, A. A. (1971). In "Techniques of Metals Research," Vol. 5, pp. 223-271. Interscience, New York.

Diesner, R. W. (1969). Society of Automotive Engineers, pamphlet 710285, SAE SP-362, X-Ray Fatigue Division.

Dietrich, G., and Potter, J. M (1977). Adv. in X-ray Analysis, 20, 321-328.

Digiacomo, G. (1969). Mater. Sci. Eng. 4, 133-145.

Doig, P., and Flewitt, P. E. J. (1977a). Phil. Mag. 35, 1063-1076.

Doig, P., and Flewitt, P. E. J. (1977b). Strain 13, 102-107.

Dolan, T. J. (1959). In "Internal Stresses and Fatigue in Metals" (G. W. Rassweiler and W. L. Grube, eds.), pp. 284-310. Elsevier Publ., New York.

Dölle, H. and Hauk, V. (1976). Härterei-Techn. Mitt. 31, 165-168.

Dölle, H. and Hauk, V. (1977). Z. Metallkunde 68, 725-728.

Dölle, H. and Hauk, V. (1978). Z. Metallkunde 69, 410-417.

Dölle, H. Hauk, V., Meurs, P., and Sesemann, H. (1976a). Metallkunde 67, 30-35.

Dölle, H., Hauk, V., Jühe, H. H., and Krause, H. (1976b). Materialprüfung 18, 427-431.

Dölle, H., Hauk, V., Kockelmann, H., and Sesemann, H. (1977). J. Strain Analysis 12, 62-65.

Donachie, M. J., and Norton, J. T. (1961). Trans. AIME 221, 962-967.

Elber, W. (1974). In "Fracture Toughness and Slow Stable Cracking" ASTM STP 559, pp. 45-58. American Society for Testing and Materials, Philadelphia, PA.

Ericsson, T., Spiegelberg, P., and Larsson, L. E. (1971). In "X-Ray Study on Strength and Deformation of Metals", p. 67-73. The Society of Materials Science, Japan.

Ericsson, T., and Hildenwall, B. (1978). Proc. AIME Annual Meeting, Denver Abstracts p. 141.

Ericsson, T., and Knuuttila, M. (1976). Second Int. Conf. on Mech. Behavior of Materials, 822-828. ASM, Metals Park, Ohio.

Esquivel, A. L. (1969). Adv. in X-ray Analysis 12, 269-298.

Esquivel, A. L., and Evans, K. R. (1968). X-Ray Diffraction Study of Residual Macrostresses in Shot Peened and Fatigued 4130 Steel, Boeing Report D6-23377.

Evans, E. B. (1969). Society of Automotive Engineers, Pamphlet 710278. SAE SP-262.

Evans, W. P., and Littman, W. E. (1963). SAE Journal, 118-121.

Evans, W. P., Ricklefs, R. E. R., and Millan, S. F. (1966). In "Local Atomic Arrangements Studied by X-Ray Diffraction" (J. B. Cohen and J. E. Hilliard, eds.), p. 351 - 377. Gordon and Breach, New York.

Evenschor, P. D., and Hauk, V. (1975a). Z. Metallkunde 66. 164-166.

Evenschor, P. D., and Hauk, V. (1975b). Z. Metallkunde 66, 167-168.

Evenschor, P. D., and Hauk, V. (1975c). Z. Metallkunde 66, 210-213.

Faninger, G. (1970). J. Soc. Mat. Sci. 19, 42-57.

Faninger, G. and Walburger, H. (1976). Härterei-Techn. Mitt. 31, 79-82.

Faninger, G. and Wolfstieg, U. (1976). Härterei-Techn. Mitt. 31, 27-32.

Flemmer, R. L. C. and Chandler, H. D. (1976). S. Afr. Mech. Eng. 26, 291-299.

French, D. N. (1969). J. Amer. Cer. Soc. 52, 271-275.

Frost, N. E., Marsh, K. J., and Pook, L. P. (1974). "Metal Fatigue." Clarendon Press, Oxford, England. p. 332-337.

Garrod, R. I., and Hawkes, G. A. (1963). Brit. J. Appl. Phys. 14, 422-428.

Giessen, W. C., and Gordon, G. C. (1968). Science 159, 973-975.

Goto, T. (1974). In "Mechanical Behavior of Materials," p. 265-278. The Society of Materials Science, Japan.

Gould, R. W., and Pittella, C. F. (1973). Adv. in X-Ray Analysis 16, 354-366.

Greenough, G. B. (1952). Prog. in Metal Physics 3, 176-219.

Grossman, L. N. and Fulrath, R. M. (1961). J. Amer. Cer. Soc. 44, 567-571.

Hammond, R. A. F., and Williams, C. (1960). Metallurgical Reviews 5, 165-223.

Hanabusa, T., Fukura, J., and Fujiwara, H. (1969). Bull. of J.S.M.E. 12, 931-939.

Hanke, E. (1969). Society of Automotive Engineers Pamphlet 710279, SAE SP-362.

Hara, A., Megata, M. and Yazu, S. (1970). Powder Met. Int. 2, 43-47.

Harterei-Techn. Mitt. (1976). 31, 1-124.

Hauk, V. and Sesemann, H. (1967). Z. Metallkunde 67, 646-650.

Hauk, V., Herlach, D., and Sesemann, H. (1976). Z. Metallkunde 66, 734-737.

Hauk, V. and Kockelmann, H. (1977). Z. Metallkunde 68, 619.

Hauk, V. and Wolfstieg, U. (1976). Härterei-Techn. Mitt. 31, 38-42.

Hawkes, G. A. (1970). J. Australian Inst. Metals 15, 157-160.

Hayama, T., and Hashimoto, S. (1975). J. Soc. Mater. Sci., Japan 23, 75-79.

Hayashi, K., and Doi, S. (1971). In "X-Ray Study on Strength and Deformation of Metals." The Society of Materials Science, Japan. p. 49-57.

Hayashi, K., Doi, S., and Natsume, Y. (1973). Society of Manufacturing Engineers Tech. Paper 1Q73-620. Dearborn, Michigan.

Hearn, E. W. (1977). Adv. in X-ray Analysis 20, 273-282.

Henriksen, E. K. (1957). Tool Engineer 38, 92-96.

Hilley, M. E., Larson, J. A., Jatczak, C. F., and Ricklefs, R. E. (eds.) "Residual Stress Measurements by X-ray Diffraction," SAE Information Report J 784a. (1971). SAE, Pennsylvania.

Hinton, R. W., Schwartz, L. H., and Cohen, J. B. (1963). J. Electrochem. Soc. 110, 103-112.

Horger, O. J. (1965). In "Metals Eng. Design," ASME Handbook, 2nd ed. McGraw-Hill, New York.

Hosokawa, N., Honda, K, and Arima, J. (1972). In "Mechanical Behavior of Materials," Vol. I, pp. 164-175. The Society of Materials Science, Japan.

Hosokawa, T., and Nobunga, S. (1969). J. Japan Soc. of Mat. Sci. 18, 24-29.

Isenburger, H. R. (1953). "Bibliography on X-Ray Stress Analysis," 2nd ed. St. John X-Ray Laboratory, Califon., New Jersey.

Ishii, K., Iwamoto, M., Shiraiwa, T. and Sakamoto, Y. (1969). Society of Automotive Engineers Pamphlet 710280. SAE SP-362.

Ivanov, S. I., and Pavlov, V. F. (1976). Strength of Materials 8, 529-531.

Iwanaga, S., Namikawa, H., and Aoyama, S. (1972). J. Soc. Mat. Sci. Japan 21, 1106-1111.

James, M. R. (1977). Ph.D. Thesis. Northwestern University, Evanston, Illinois.

James, M. R., and Cohen, J. B. (1976). Adv. in X-Ray Analysis 19, 695-708.

James, M. R., and Cohen, J. B. (1977). Adv. in X-Ray Analysis 20, 291-308.

James, M. R., and Cohen, J. B. (1978). J. of Testing and Evaluation 6, 91-97.

James, M. R., and Cohen, J. B. (1979). J. Appl. Cryst.

Jatczak, C., and Boehm, H. (1973). Adv. in X-Ray Analysis 17, 354-362.

Kamachi, K. (1971). In "X-Ray Study on Strength and Deformation of Metals." The Society of Mat. Sci., Japan. p. 95-104.

Kamachi, K., and Kawabe, Y. (1976). Proc. of the Second International Conference on Mechanical Behavior of Materials (ASM), 1604-1608.

Kawai, K., and Takizawa, Y. (1974). In "Mechanical Behavior of Materials," The Society of Materials Science, Japan. p. 309-317.

Kelly, C. J., and Eichen, E. (1973). Adv. in X-ray Analysis 16, 344-353.

Kelly, C., and Short, M. A. (1970). Adv. in X-ray Analysis 114, 377-387.

Kempel, E. (1971). J. Basic Engineering, Trans. Amer. Soc. Mech. Eng. 93, 317.

Keng, W., and Weil, R. (1971). Acta Cryst. 27A, 578-585.

Kirk, D. (1971). Strain 7, 7-14.

Kirk, D., Nelms, P. R., and Arnold, B. (1966). Metallurgia 74, 255-257.

Klug, H. P., and Alexander, L. E. (1974). In "X-Ray Diffraction Procedures," pp. 755-790. John Wiley and Sons, Inc., New York.

Kodama, S. (1971). In "X-Ray Study on Strength and Deformation of Metals," p. 43-48. The Society of Materials Science, Japan.

Kodama, S. (1972). In "Mechanical Behavior of Materials," p. 111-118. The Society of Materials Science, Japan.

Koistinen, D. P. (1958) Trans. ASM. 50, 227-241.

Koistinen, D. P., and Marburger, R. E. (1959). Trans. ASM. 51, 537-555.

Koistinen, D. P., and Marburger, R. E. (1959). In "Internal Stress and Fatigue in Metals" (G. M. Rassweiller and W. L. Grube, eds.), pp. 110-119.

Elsevier Publ. Co., New York.

Kornev, A. D., Vorob'ev, G. M., and Shmyreva, T. P. (1976). Strength of Materials 8, 449-451.

Koster, W. P., Field, M., Fritz, L. J., Gatto, L. R., and Kahles, J. R. (1970). Technical Report AFML-TR-70-11, U.S. Air Force Materials Laboratory.

Koves, G. (1965). Adv. in X-ray Analysis 9, 468-486.

Koves, G., and Ho, C. Y. (1964). Norelco Reporter XI, 99.

Kraus, I., and Nehasil, M. (1976). Strojirenstvi 26, 485-486.

Krause, H. and Jühe, H. H. (1976). Härterei-Techn. Mitt. 31, 168.

Krause, H., and Jühe, H. H. (1977). Wear 36, 15-21.

Krause, R. F., and Cullity, B. D. (1968). J. Appl. Phys. 39, 5532-5537.

Kuruzar, M. E., and Cullity, B. D. (1971). Inter. J. Magnetism 1, 323-325.

Ladell, J., Parrish, W., and Taylor, J. (1959). Acta Cryst. 12, 561-570.

Landgraf, R. W. (1973). American Society for Testing Materials, ASTM STP-519, 213.

Larson, L. E. (1974). J. Metallurgy 3, 119-122.

Lei, T. S., and Scardina, J. T. (1976). In "Microstructural Science," 4, 269-280. Elsevier Pub. Co., New York.

Leonard, L. (1973). ONR TRF-C3454, The Franklin Institute, Philadelphia, PA.

Lessells, J. M. and Brodrick, R. F. (1956). Proc. Inter. Conf. on Fatigue of Metals, London, 617-627.

Lester, H. H., and Aborn, R. H. (1925-26). Army Ordinance 6, 120, 200, 283, 364.

Leverant, G. R., Langer, B. S., Yuen, A., and Hopkins, S. W. 1978. Met. Trans., in press.

Liss, R. B., Massiron, C. G., and McKloskey, A. S. (1966). SAE Trans. 74, 870-877.

MacDonald, B. A. (1970). Adv. in X-Ray Analysis 13, 487-506.

MacGillavary, C. H., and Rieck, G. D. (eds.) (1968). "International Tables for X-Ray Crystallography." Kynoch Press, England.

Macherauch, E. (1961). Proc. of the 3rd Int. Conf. on Nondestructive Testing, Tokyo, Japan, pp. 727-733.

Macherauch, E. (1966). Exp. Mech. 6, 140-153.

Macherauch, E. and Müller, D. (1961). Z. Angew. Physik. 13, 305.

Macherauch, E. and Wolfstieg, U. (1977). Adv. in X-Ray Analysis 20, 369-377.

Macherauch, E., and Wolfstieg, U. (1977). Materials Science and Engineering 30, 1-13.

Marburger, R. E. and Koistinen, D. P. (1961). Trans. ASM 53, 743-752.

Marion, R. H. (1972). Ph.D. Thesis. Northwestern University, Evanston, Illinois.

Marion, R. H., and Cohen, J. B. (1974). Adv. in X-Ray Analysis 18, 466-501.

Marion, R. H., and Cohen, J. B. (1977). Adv. in X-Ray Analysis 20, 355-368.

Marschall, C. W., and Maringer, R. E. (1977). In "Dimensional Instability," Chap. 6. 139-211. Pergamon Press, London.

McClintock, F. A., and Argon, A. S. (1966). In "Mechanical Behavior of Materials," pp. 420-442. Addison Wesley, Mass.

Mitchell, C. M. (1977). Adv. in X-Ray Analysis 20, 379-392.

Möller, H., and Martin, G. (1939). Mitt. Aus. der Kaiser-Wihelm-Institute für Eisenforschung 21, 261-269.

Morrow, J., Ross, A. S., and Sinclair, G. M. (1960). SAE Trans. 68, 40-48.

Motoyama, M., and Horisawa, H. (1969). Society of Automotive Engineers, Pamphlet 710281, SAE SP-361.

Muro, H., and Tokuda, M. (1968). J. Soc. Mat. Sci., Japan 17, 1094-1097.

Muro, H., Tsushima, N., and Nunome, K. (1973). Wear 25, 345-356.

Nagao, M. and Kusumoto, S. (1976). Proc. Second Inter. Conf. on Mech. Behavior of Materials, ASM, pp. 1609-1613.

Nagao, M. and Weiss, V. (1977). Trans. ASHE - J. Eng. Mater. and Tech. 99, 110-113.

Nakagawa, Y. and Tamamura, T. (1974). In "Mechanical Behavior of Materials." The Society of Materials Science Japan. pp. 297-308.

Nakagawa, Y., Tamamura, T., and Nemoto, T. (1972). J. Soc. Mat. Sci., Japan 21, 1099-1105.

Nelson, D. V., Ricklefs, R. E., and Evans, W. P. (1969). Society of Automotive Engineers, Pamphlet 710283, SAE SP-362.

Nelson, D. V., Ricklefs, R. E., and Evans, W. P. (1970). In "Achievements of High Resistance in Metals and Alloys," p. 228-253. ASTM STP 467, ASTM, Philadelphia, PA.

Nolke, H., and Speicher, V. (1973). Härterei-Tech. Mitt. 28, 293-296.

Norton, J. T. (1967). Adv. in X-Ray Analysis 11, 401-409.

Oda, A., and Miyagawa, H. (1976). J. Soc. Mat. Sci. 25, 13-19.

Oyane, M., and Kojima, K. (1955). JSME 21, 817-836.

Parlane, A. J. A. (1977). "Residual Stresses in Thick Weldments - A Review of Contemporary Measurements Techniques." The Welding Institute Research Lab., Cambridge, England.

Pattinson, E. J., and Dugdale, D. S. (1962). Metallurgia 66, 228-230.

Peiter, A. (1976). Härterei-Techn. Mitt. 31, 158-165.

Pike, E. R., and Wilson, A. J. C. (1959). Brit. J. Appl. Phys. 10, 57-68.

Potter, J. M. (1972). ASTM-STP 519, American Society for Testing and Materials, Philadelphia, PA. pp. 109-132.

Potter, J. M., and Millard, R. A. (1977). Adv. in X-Ray Analysis 20, 309-320.

Prümmer, R. (1967). Ph.D. Dissertation. University of Karlsuhre.

Prümmer, R. (1970). Proc. 6th Inter. Conf. on Nondestructive Testing, Hanover, Germany.

Prümmer, R., and Macherauch, E. (1965). Naturforschg. 20A, 1369-1370.

Prümmer, R., and Macherauch, E. (1966). Z. Naturforschg. 21A, 661-662.

Prevey, P. S. (1976). Adv. in X-ray Analysis 19, 709-724.

Prevey, P. S. (1977). Adv. in X-ray Analysis 20, 345-354.

Prevey, P. S., and Field, M. (1975). Annals. of CIRP 24, 497-501.

Quesnel, D. J., Meshii, M., and Cohen, J. B. (1978). Mat. Sci. and Eng. In press.

Radhakrishnan, V. M. and Prasad, C. R. (1976). Eng. Frac. Mech. 8, 593-597.

Ranganathan, B. N., Wert, J. J. and Clotfelter, W. N. (1976). J. Test. Eval. 4, 218-219.

Rassweiller, G. M., and Grube, W. L. (eds.). (1959). "Internal Stresses and Fracture in Metals." Elsevier Pub. Co., New York.

Revay, L. (1975). Electrodeposition Surf. Treat. 3, 94-104.

Ricklefs, R. E., and Evans, W. P. (1966). Adv. in X-Ray Analysis 10, 273-283.

Rimrott, F. P. S. (1962). Design Engineering 8, 48-50.

Robertson, G. T. (1969). Society of Automotive Engineers, Pamphlet 710284, SAE-SP-362.

Rosenthal, D. (1959). In "Metal Fatigue" (G. Sines and J. L. Waisman), p. 170. McGraw-Hill, New York.

Rozgonyi, G. A., and Ciescielka, T. J. (1973). Rev. Sci. Instr. 44, 1053-1057.

Rozgonyi, G. A., and Miller, D. C. (1976). Thin Solid Films 31, 185-216.

Rutledge, A. L., and Taylor, R. M. (1972). J. Strain Analysis 7, 1-6.

Schaaber, O. (1939). Z. Tech. Phys. 20, 264.

Schmidt, W. (1976). VDJ Z. 118, 1023-1027, 1123-1127.

Schulz, L. G. (1949). J. Appl. Phys. 20, 1030-1033.

Senatorova, O. G., and Samoilov, A. I. (1969). Metal Science and Heat Treatment, No. 4, April 1969, 322-324.

Seppi, F. L. (1976). Proc. of a Workshop on Nondestructive Evaluation of Residual Stress, NTIAC-76-2. pp. 73-76. Southwest Research Institute, San Antonio, Texas.

Shiraiwa, T., and Sakamoto, Y. (1970). Proc. of the Thirteenth Japan Congress on Materials Research, pp. 25-32.

Shiraiwa, T., and Sakamoto, Y. (1971). In "X-Ray Study on Strength and Deformation of Metals." The Society of Materials Science, Japan. p. 15-22.

Shiraiwa, T., and Sakamoto, Y., (1972). Sumitomo Search 7, 109.

Shiraiwa, T., and Sakamoto, Y. (1973). SME Tech. Paper No. IQ73-621, Society of Automotive Engineers, Dearborn, Michigan.

Short, M. A. and Kelly, C. J. (1973). Adv. in X-Ray Analysis 16, 379-385.

Singh, A. K. and Balasingh, C. (1971). J. Appl. Phys. 42, 5254-5260.

Singh, B., Lewis, D., Towner, J. M., Waldron, M. B., and Lee, J. R. (1973). In "Titanium Science and Technology," Vol. 1, pp. 743-745. Plenum Press,

Smith, S. L., and Wood, W. A. (1944). Proc. Roy. Soc. A. 182, 404-415.

Snyder, H. J. (1952). Trans. ASM. 45, 605-619.

Society of Automotive Engineers. (1978). "SAE Handbook," Pt. I. Society of Automotive Engineers, New York. p. 443.

Society of Materials Science. (1973). "Standard Method for X-Ray Stress Measurement." The Society of Materials Science, Japan.

Society of Materials Science. (1974). "X-Ray Studies on Mechanical Behavior of Metals." The Society of Materials Science, Japan. pp. 72-132.

Spiriana, S. I., Sverdlova, B. M., and Spirina, N. I. (1975). Strength of Materials 7, 1105-1111.

Steffan, A. and Ruud, C. A. (1978). Adv. in X-Ray Analysis 21, 309-315.

Stroppe, H. (1963). Wiss. Z. Th.Otto V. Guericke Magdeburg 7, 345.

Syren, B., Wohlfahrt, H. and Macherauch, E. (1976a). Härterei-Tech. Mitt 31, 90-94.

Syren, B., Wohlfahrt, H., and Macherauch, E. (1976b). Second Int. Conf. on Mech. Behavior of Materials, 807-811.

Taira, S., and Hayashi, H. (1970). Proc. of the Thirteenth Japan Congress on Materials Research. pp. 20-24.

Taira, S., and Hayashi, K. (1971). In "Mechanical Behavior of Metals" Vol. I, pp. 152-163. The Society of Materials Science, Japan.

Taira, S., and Matsuki, K. (1968). J. Soc. Mat. Sci. 17, 1053-1058.

Taira, S., Abe, T., and Ehiro, T. (1969). J. Soc. Mat. Sci. 12, 53,947-957.

Taira, S., Hayashi, K., and Watase, Z. (1969). Proc. of the Twelfth Japan Congress on Materials Research. pp. 1-7.

Taira, S., Hayashi, K., and Ozawa, S. (1974). In "Mechanical Behavior of Metals," pp. 287-295. The Society of Materials Science, Japan.

Takada, H., and Matsumoto, M. (1976). Second International Conference on Mechanical Behavior of Materials (ASM). pp. 1619-1623.

Tarasov, L. P., Hyler, W. S., and Letner, H. R. (1957). Proc. ASTM. 57, 601-622.

Thomsen, J. S., and Yap, F. Y. (1968). J. of Research of Nat. Bureau of Stan. 72A, 187-204.

Turovskii, M. L., Belozerov, V. V., Shifrin, I. S., and Fuks, M. Y. (1976). Strength of Materials 8, 104-109.

Underwood, J. H., Pook. L. P., and Sharples, J. K. (1977). In "Flaw Growth and Fracture," ASTM STP 631, pp. 402-415. American Society for Testing and Materials, Philadelphia, Pennsylvania.

Valorinta, V. (1965). Metal Treatment 32, 322-329.

Weidemann, W. (1966). Ph.D. Thesis. Technische Hochschule, Aachen, West Germany.

Weinman, E. W., Hunter, J. E., and McCormack, D. D. (1969). Metal Progress 96, 88-91.

Weissmann, S., and Saka, T. (1977). Adv. in X-Ray Analysis 20, 237-244.

Wheeler, D. R. (1974). Tech. Report NASA-TN-D-7578. NASA Lewis Research Center, Cleveland, Ohio.

Wilson, A. J. C. (1967). Acta Cryst. 23, 888-898.

Wohlfahrt, M. (1973). Härterei-Tech. Mitt. 28, 288-293.

Wohlfahrt, M. (1976). Härterei-Tech. Mitt. 31, 56-71.

Wolfstieg, U. (1959). Arch. Eisenhüttenwes. 30, 447.

Wolfstieg, U. (1976). Härt-Techn. Mitt. 31, 33-37.

Wolfstieg, U., and Macherauch, E. (1976). Härt. Techn. Mitt. 31, 2-3.

Wolt, H., Stucher, E. S., and Nowach, N. (1977). Arch. Eisenhüttenwes. 48, 173-178.

Yoshioka, Y. (1976). J. Soc. Mater. Sci., Japan 25, 1-5.

Zantopulos, H., and Jatczak, C. F. (1970). Adv. in X-Ray Analysis 14, 360-376.

Ziegeldorf, S . (1976). Dissertation. Tech. Univ. München.

Table I

Classification of Internal Stresses*

Range	Sums to zero	Kind	Effects on Diffraction Pattern	Examples of the Source
(mm) Macroscopic	over the sample	1st	Peak Shift	Machining stresses, thermal stresses, assembly stresses
(μm) Microscopic over grains	over several grains	2nd	Peak Shift and Peak Broadening	Particles of different phases or yield strengths than the matrix
(1 - 1000 Å) within grains	within a grain	3rd	Peak Broadening	Edge and screw dislocation

*Adapted from Buck and Thompson, 1977.

TABLE II

FACTORS WHICH INFLUENCE ACCURACY AND PRECISION IN X-RAY STRESS MEASUREMENT*

Instrumental and Equipment	Geometrical	Specimen
Alignment of diffractometer	Radiation	Type of Material
Specimen Alignment	{hkℓ} Planes	Crystal System
θ/2θ Relationship	Apertures	Technique of Specimen Preparation
Parafocussing	Technique of Beam Focussing	Specimen Size and Geometry
Apertures	LP and Absorption Effects	Elastic Constants
Soller Baffles	Counting Statistics	Mass Absorption Coefficients
Detector	Scanning Method	Grain Size
Radiation	Method of Stress Calibration	Effect of Other Phases
Noise Discrimination	Deviation from Plane Stress	Type of Deformation Producing Stress
Power Stability	Corrections for Beam Penetration	Stacking Faults
Detector Stability	Corrections for Material Removal	Twinning
		Texture

*After Jatczak and Boehm (1973).

TABLE III

CHANGE IN CORRECTION FACTORS FROM 154° TO $158^{\circ}2\theta$

FOR UNPOLARIZED Fe AND CrK_{α} RADIATION*

Term	$2\theta=154^{\circ}$	$2\theta=158^{\circ}$	Difference
Lorentz factor ($1/\sin^2\theta$)	1.0533	1.0378	- 1.47%
Polarization factor ($1+\cos^2 2\theta$) (unpolarized incident beam)	1.8078	1.8596	+ 2.87%
Absorption at $\psi = 0^{\circ}$	1.	1.	0
Absorption at $\psi = 45^{\circ}$	0.7691	0.8056	+ 4.74%
Atomic scattering factor (f^2)	1.3503	1.3322	- 1.34%
Temperature factor (e^{-M})	0.8653	0.8634	- 0.22%

*After Short and Kelly (1973)

TABLE IV

TYPICAL INSTRUMENTATION ERRORS IN PEAK LOCATION FOR $2\theta = 156^{\circ}$

(Approximately the 211 CrK_{α} Peak from Iron)

Cause	Peak shift between $\psi = 0^{\circ}$ and $\psi = 45^{\circ}$	Peak shift between $\psi = 0^{\circ}$ and $\psi = 60^{\circ}$
Peak Location, $\pm 0.01^{\circ} 2\theta$	$\pm 0.02^{\circ} 2\theta$	$\pm 0.02^{\circ} 2\theta$
Horizontal beam divergence ($\alpha = .5^{\circ}$) (Taking $1/2(\delta(\Delta 2\theta)_{BD})$ see Eq. 24	$-.0006^{\circ}$ 2θ	$-.0025^{\circ}$ 2θ
Vertical beam divergence (Assuming strong texture using divergent Soller slit; no receiving Soller slit)	$-.002^{\circ}$ 2θ or $+.002^{\circ}$ 2θ	$-.002^{\circ}$ 2θ or $+.002^{\circ}$ 2θ
Sample displacement, $\Delta x = \pm .025$ mm	$-.0034^{\circ}$ 2θ or $+.0034^{\circ}$ 2θ	$-.0088^{\circ}$ 2θ or $+.0088^{\circ}$ 2θ
ψ-axis displacement, $\Delta x' = \pm .025$ mm	$-.002^{\circ}$ 2θ or $+.002^{\circ}$ 2θ	$-.0068^{\circ}$ 2θ or $+.0068^{\circ}$ 2θ
Maximum total errors*+ a) in -2θ direction b) in $+2\theta$ direction	$-.008^{\circ}$ 2θ $+.0068^{\circ}$ 2θ	$-.0201^{\circ}$ 2θ $+.0149^{\circ}$ 2θ
Maximum error in stress for steel†	-4.74 MPa (-690 psi) or +4.0 MPa (-585 psi)	-7.0 MPa (-1150 psi) or +5.9 MPa (+860 psi)

*Note: Maximum error is either one of these but not the total range.

†Calculated for steel from $\sigma_{\varphi} = K_{\psi}(2\theta_{\perp} - 2\theta_{\psi})$ where $K_{45} = 593$ MPa/$^{\circ}2\theta$ and $K_{60} = 396$ MPa/$^{\circ}2\theta$. Does not include error in peak location as it is dependent on time of data collection.

TABLE V

PRECISION OF VARIOUS MEASURES OF PROFILE POSITION

(10 measurements with a PSD, many points in the profile)

Steel	FWHM* ($^{o}2\theta$)	Half-Value Breadth ($^{o}2\theta$)	Centroid ($^{o}2\theta$)	Parabola ($^{o}2\theta$)
†1090	.45	156.149 (± .021)**	156.096 (± .011)	156.186 (± .016)
††1045	3.45	155.336 (± .064)	155.396 (± .085)	155.413 (± .020)

*FWHM is the full width at half of the maximum intensity.

†Air co led from 820°C, then stress relieved by slow cooling from 677°C to produce a sharp profile.

**The term in ( ) represents one standard deviation from the average position over the 10 measurements.

††Oil quenched from 820°C, tempered at 378°C, 1 hr., shot peened to produce a broad profile and a peak/background ratio of only 1.6.

TABLE VI

DIFFRACTION PLANE DEPENDENCE OF STRESS IN THREE PLASTICALLY DEFORMED Fe BASED MATERIALS

(Measured x-ray elastic constants were employed. From Marion and Cohen, 1977)

Sample	Deformation	Stress (MPa)	
		211 CrK_α peak	310 CoK_α peak
AISI 1045	13% Tensile	-212.0	-318.3

LIST OF FIGURE CAPTIONS

Fig. 1 The symbols and axes employed in measurement of residual stresses with x-rays.

Fig. 2 (a) Schematic of a diffractometer. The incident beam diffracts x-rays of wavelength λ from planes that satisfy Bragg's law, in crystals with these planes parallel to the sample's surface. The diffracted beam is recorded as intensity vs. scattering angle by a detector moving with respect to the specimen. If the surface is in compression, because of Poisson's effect these planes are further apart than in the stress-free state. Their spacing (d) is obtained from the peak in intensity versus scattering angle 2θ and Bragg's law, $\lambda = 2d\sin\theta$.

(b) After the specimen is tilted, diffraction occurs from other grains, but from the same planes, and these are more nearly perpendicular to the stress. These planes are less separated than in (a). The peak occurs at higher angles, 2θ.

(c) After the specimen is tilted, the stress is measured in a direction which is the intersection of the circle of tilt and the surface of the specimen.

Fig. 3 Angles in single exposure method. The angles η_1 and η_2 define the peak shift. The term β defines the angle between the surface normal and the primary beam.

Fig. 4 Stress constant K as a function of angle for the single

exposure and two-tilt method.

Fig. 5 Geometry of a Bragg-Brentano powder diffractometer. Note how the radius of the focusing circle decreases with increasing 2θ, and that the specimen (S) rotates θ, when the detector (C) rotates 2θ.

Fig. 6 The omega diffractometer. The ψ tilt is around an axis perpendicular to the drawing. The source (S), slits (C), detector (D), and specimen are all on one focusing circle (shown dotted in (a)) in the $\psi = 0$ position, but the focus moves when the specimen is tilted ψ as in (b). In the stationary slit method, the detector and slit remain at D, whereas in the parafocusing method the slit is moved to C in (b).

Fig. 7 The parallel beam method. The dashed horizontal lines represent various positions for the specimen. Note that since the angle between the incident and scattered beams is defined by the Soller slits, all these positions yield the same 2θ.

Fig. 8 Illustration of the effect of sample displacement (Δx) on the peak position when the sample is tilted ψ degrees.

Fig. 9 The ψ diffractometer. Note that the ψ tilt is around an axis in the plane defined by the incident and scattered x-ray beams.

Fig. 10 "PARS" (Portable Analyzer for Residual Stresses) in use by one of the authors (M.J.)

Fig. 11 Departure from ideal focusing condition. The intersection of the left, L, right, R, and center, C, rays are shown in b. The focus is not a point for a flat sample.

Fig. 12 Illustration of the effect of ψ rotation axis not coincident with the 2θ axis (point A is the 2θ axis and point 0 is the ψ axis).

Fig. 13 Effect of correction factors on the stress profile for a light peened sample, $\psi = 0^{\circ}$, and 60°, 6061-T6 Al alloy (from Lei and Scardina (1976)). Reprinted with permission of the authors and American Elsevier Publishing Co.

Fig. 14 Four types of possible lattice strain distributions (vs $\sin^2\psi$).

Fig. 15 (a) "d" vs $\sin^2\psi$ for an Armco Iron specimen reduced 69 pct by rolling; 211 peak, CrK_α. $\varphi = 0^{\circ}$. ——— curve through experimental points. --------σ_φ +9MPa using the method of Marion and Cohen (1975).

(b) Texture (integrated peak intensity) for (a).

Fig. 16 Stresses vs depth after quenching and tempering plain carbon and boron-containing steels of approximately equal carbon content and hardness. Reprinted with permission of the American Society for Testing and Materials (Copyright, 1971) and the authors; from Nelson, Ricklefs and Evans (1970).

Fig. 17 Residual stress induced by shot peening vs depth below the surface in SAE 5160 steel ($R_c = 50$). The small shot size is CS230, the large size is CS660. Reprinted with permission of SAE, Inc. and the author; from Robertson (1969).

Fig. 18 The effect of hardness on stress distribution, SAE 4340 steel, R_c = 31 and 52, curve A. Curve B: after peening R_c = 31 specimen. Curve C: after peening R_c = 52 specimen. (Shot diameter and shot size identical in B and C.) Reprinted by permission of the Council of the Institution of Mechanical Engineers, from Lessells and Brodrick (1956).

Fig. 19 Hoop stress at cold worked holes with various permanent interferences. Reprinted with permission of the authors and Plenum Publishing Corp. From Dietrich and Potter (1977).

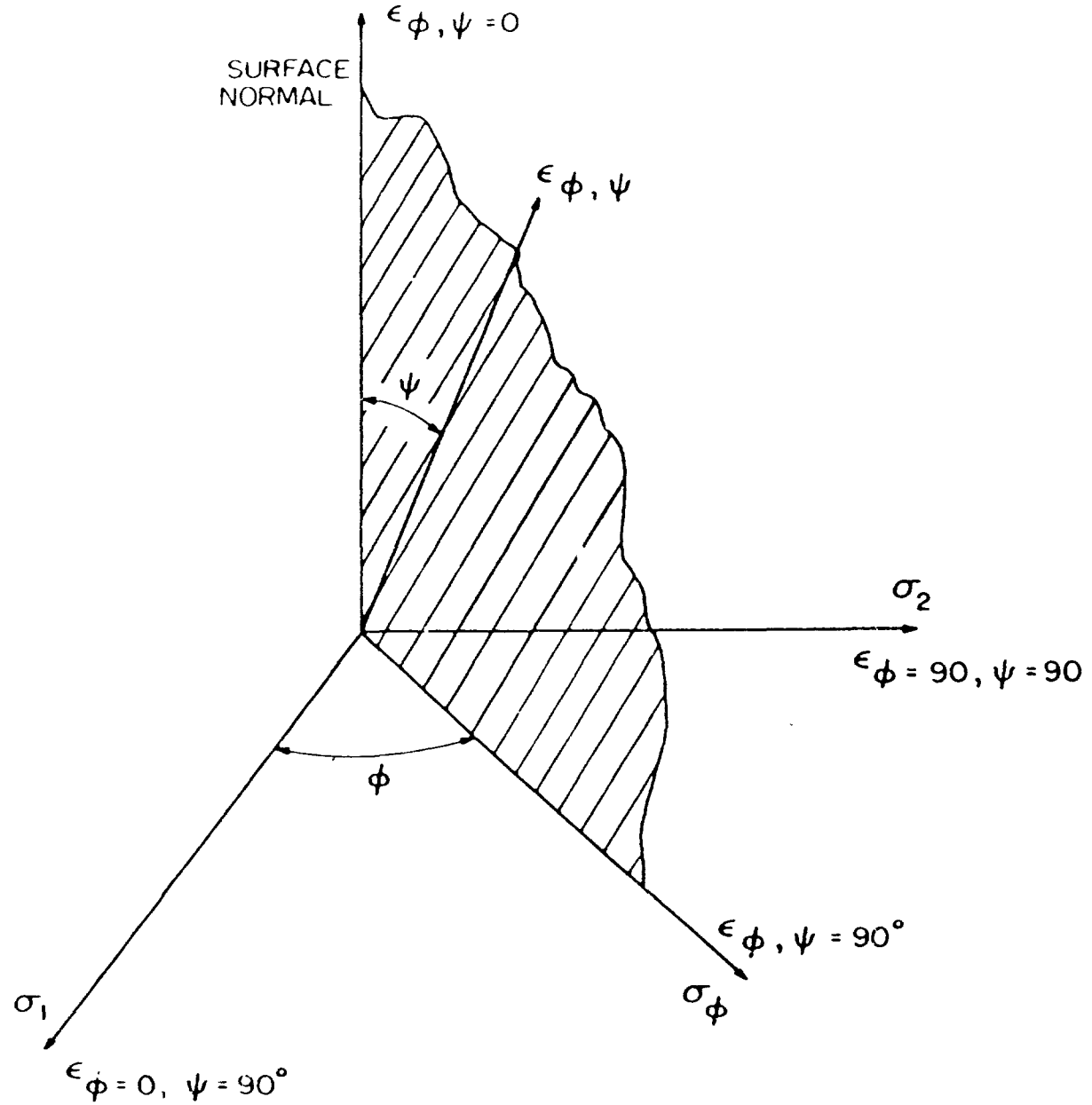
$\epsilon_{\phi,\psi=0}$
SURFACE NORMAL
$\epsilon_{\phi,\psi}$
ψ
σ_2
$\epsilon_{\phi=90,\psi=90}$
ϕ
$\epsilon_{\phi,\psi=90°}$
σ_ϕ
σ_1
$\epsilon_{\phi=0,\psi=90°}$

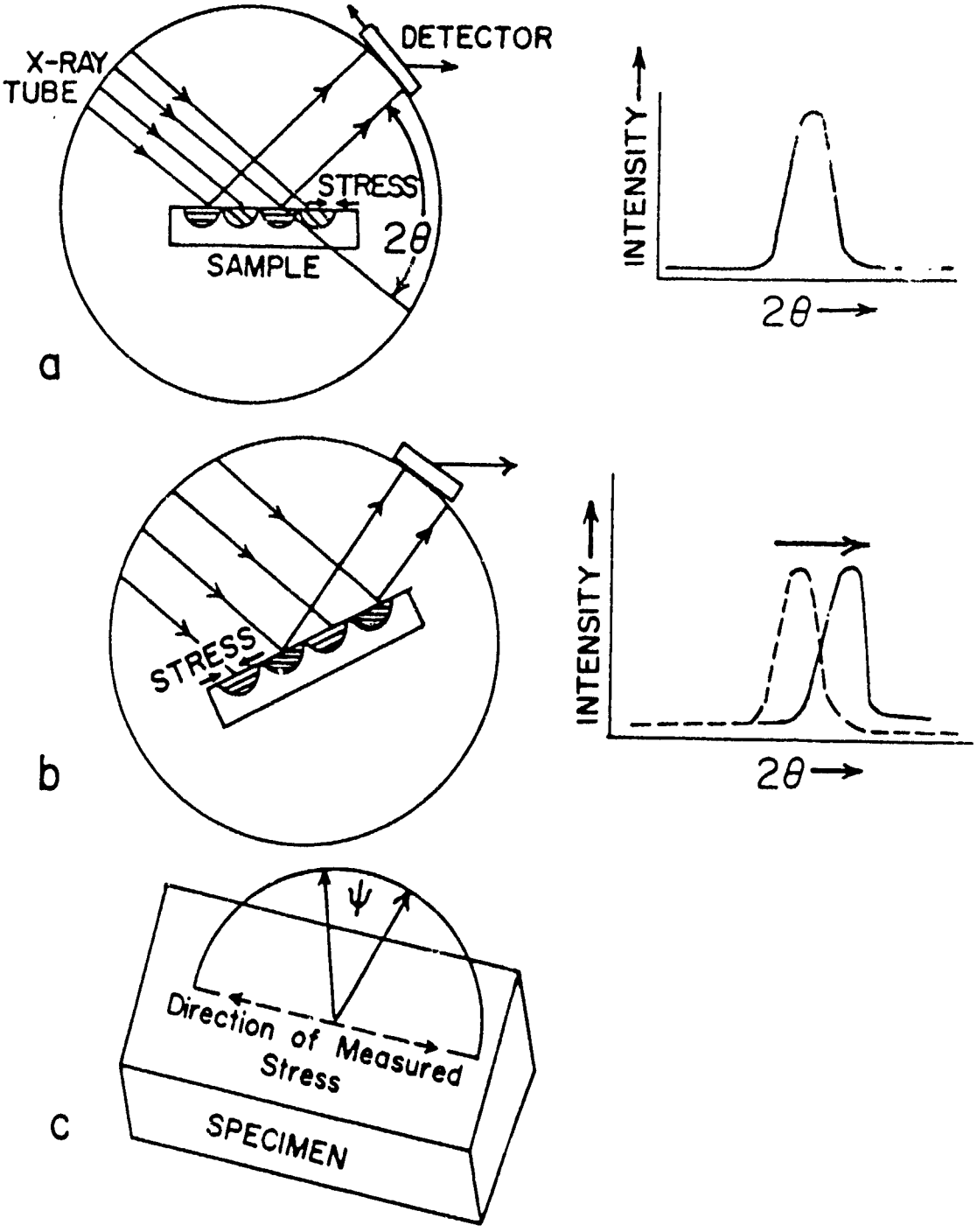
X-RAY
TUBE
DETECTOR
STRESS
SAMPLE
2θ
a
INTENSITY
2θ
b
STRESS
INTENSITY
2θ
ψ
Direction of Measured
Stress
SPECIMEN
c

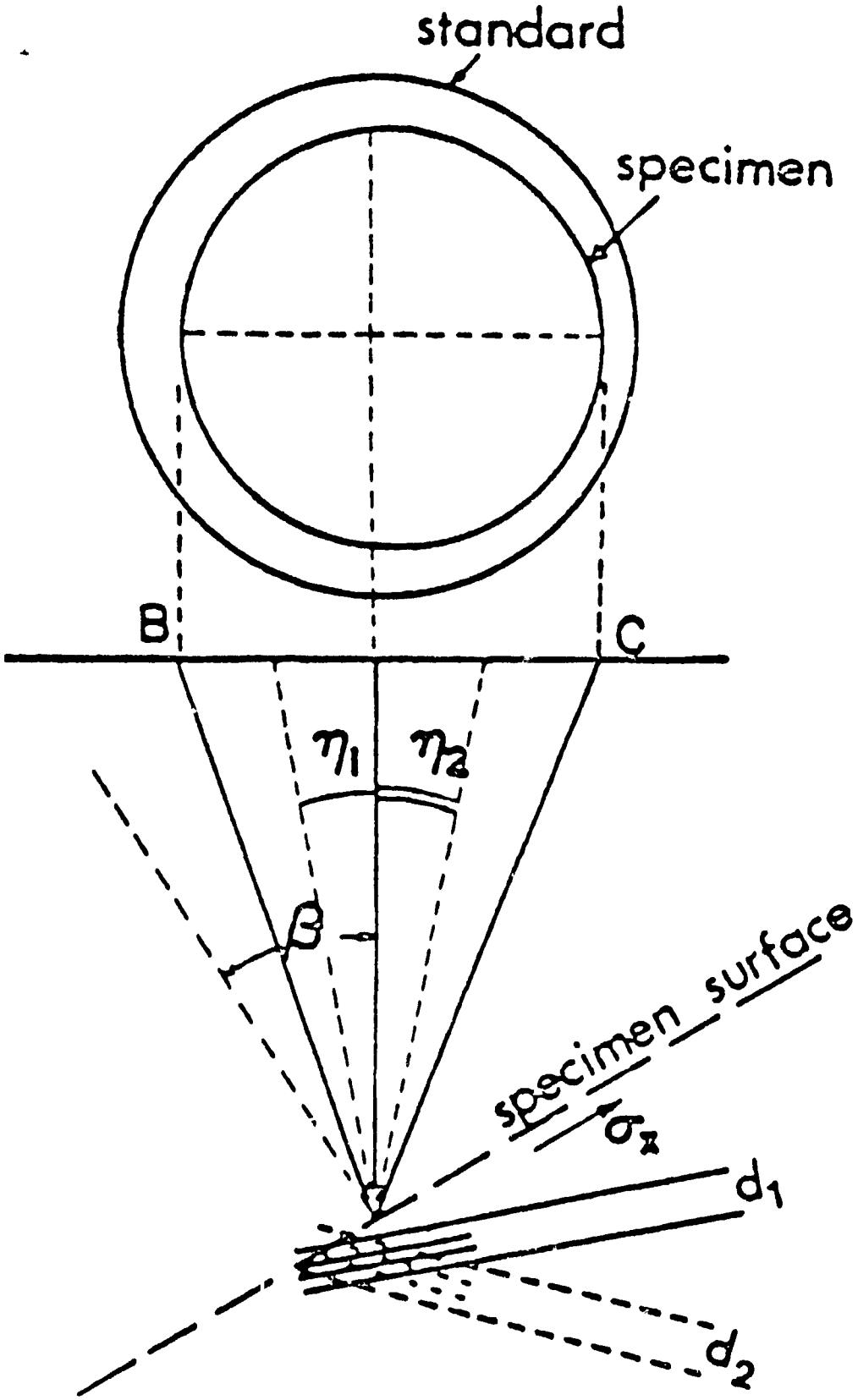
standard
specimen
B
C
η_1
η_2
β
specimen surface
σ_x
d_1
d_2

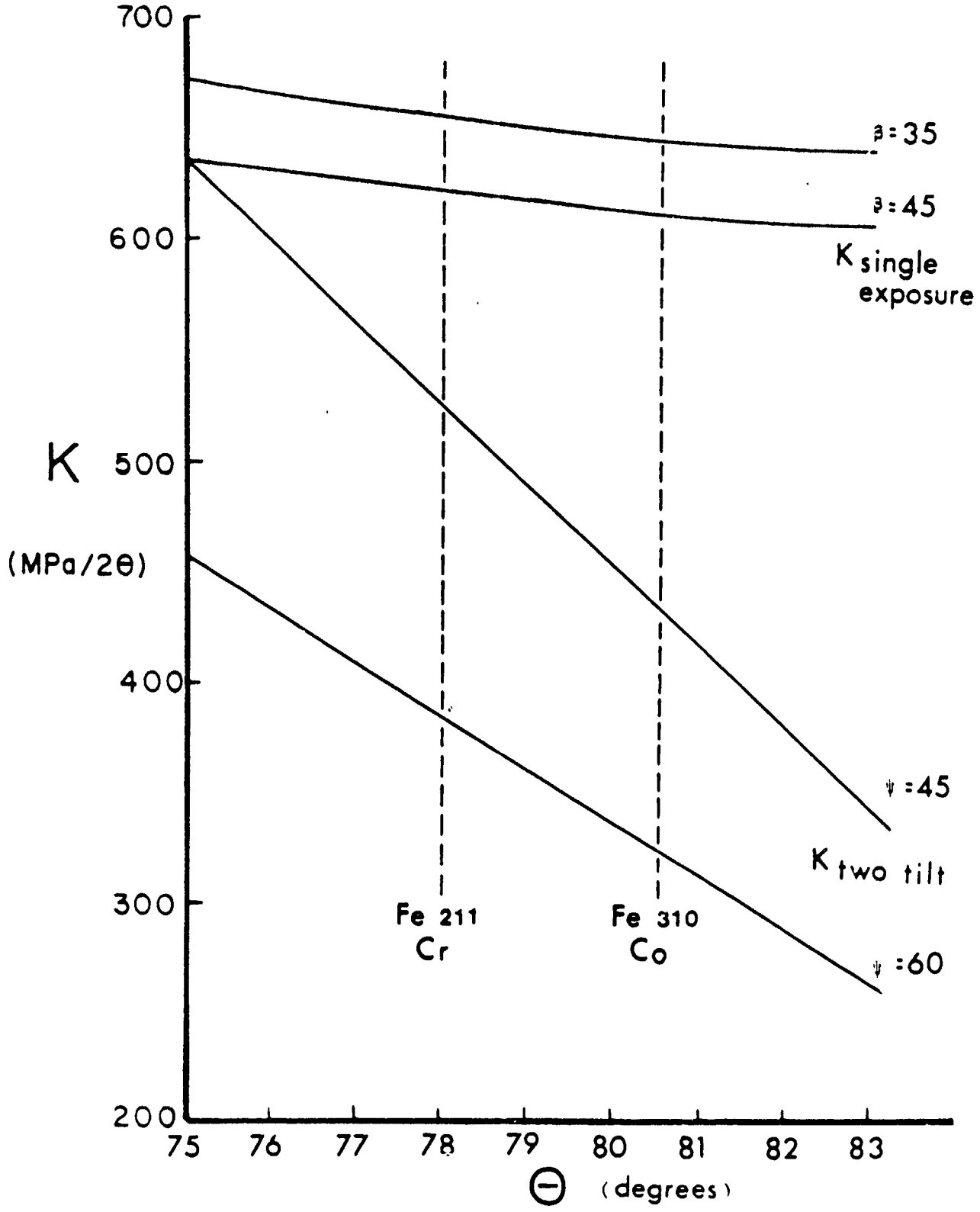
700
600
500
400
300
200
K
(MPa/2θ)
ψ=35
ψ=45
K single exposure
ψ=45
K two tilt
ψ=60
Fe 211
Cr
Fe 310
Co
75
76
77
78
79
80
81
82
83
Θ (degrees)

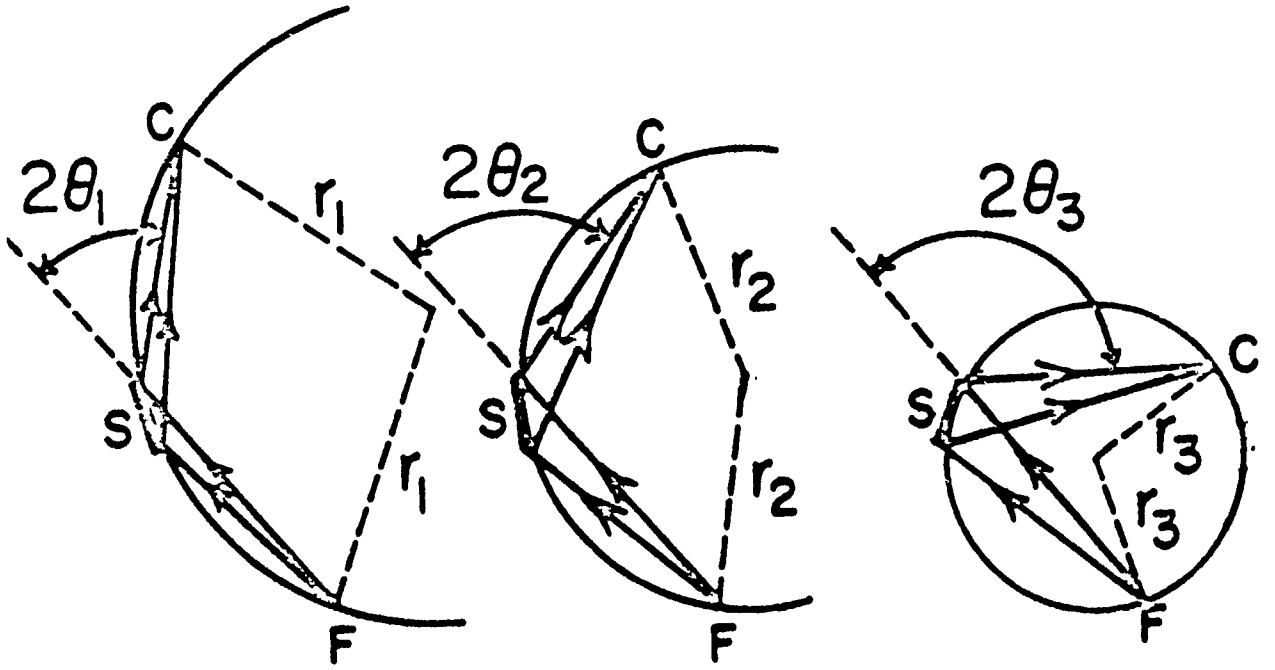
C
$2\theta_1$
r_1
S
r_1
F
C
$2\theta_2$
r_2
S
r_2
F
$2\theta_3$
C
S
r_3
r_3
F

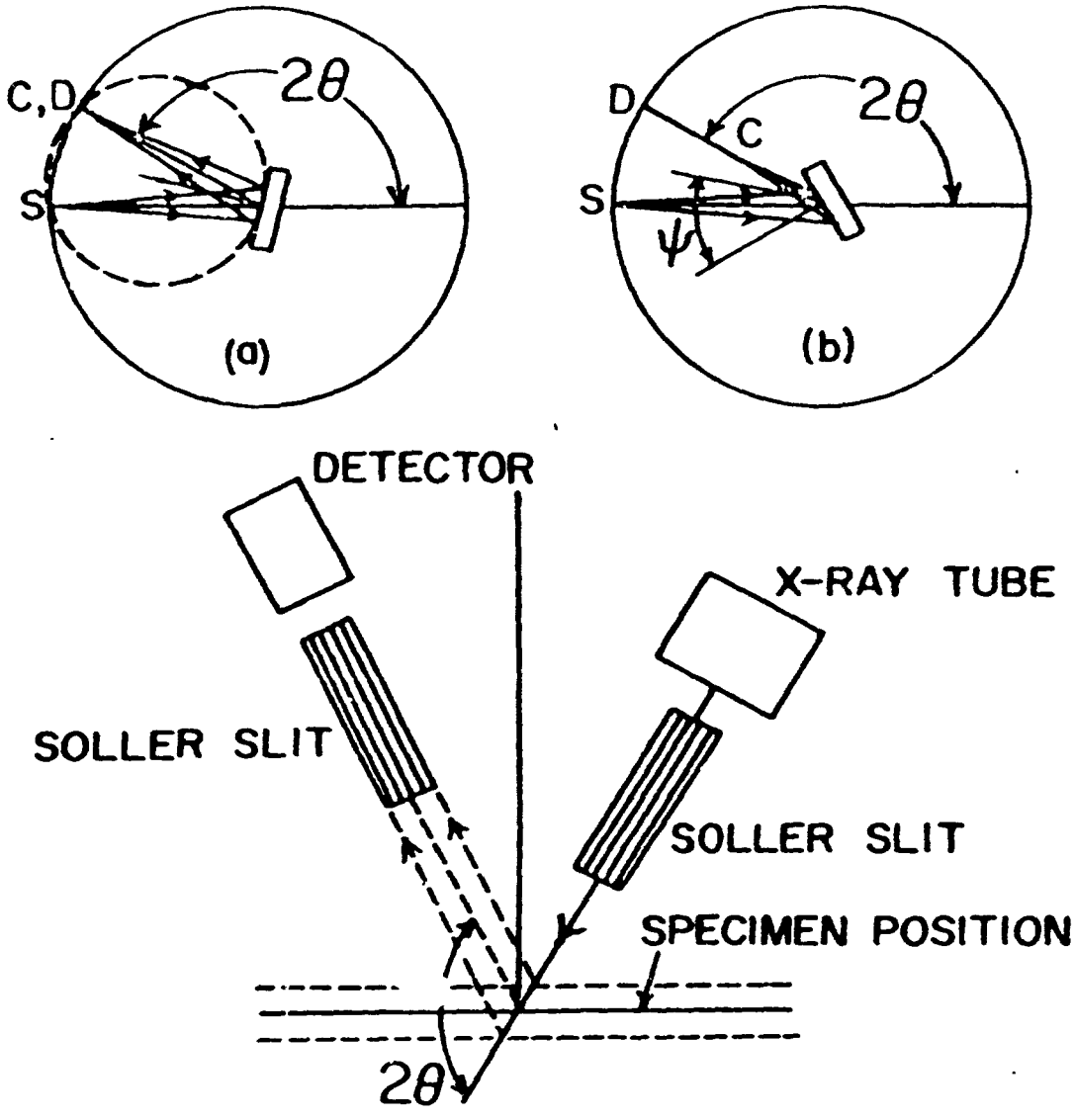
C,D
2θ
S
(a)
D
C
2θ
S
ψ
(b)
DETECTOR
X-RAY TUBE
SOLLER SLIT
SOLLER SLIT
SPECIMEN POSITION
2θ

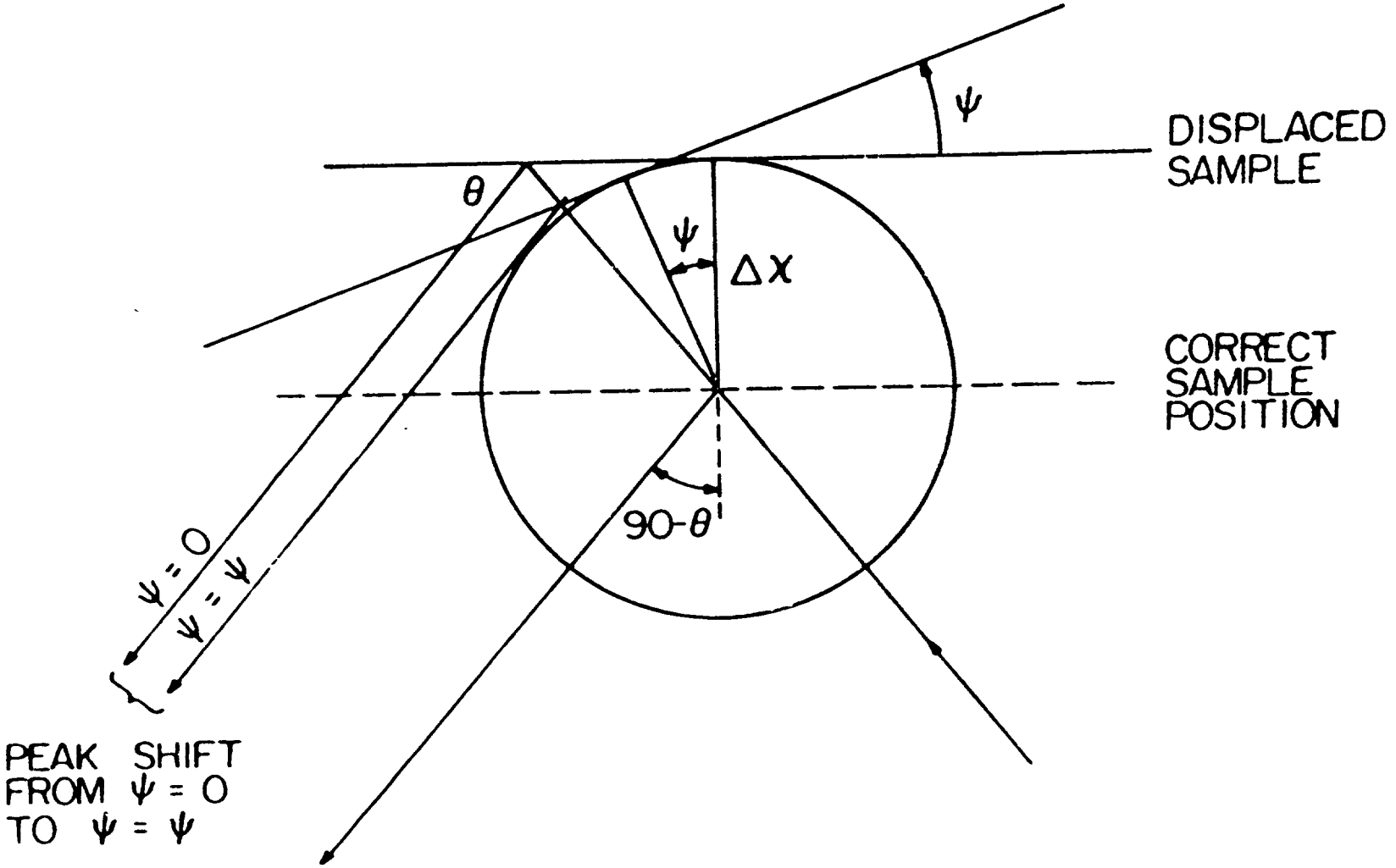
ψ
DISPLACED SAMPLE
θ
ψ
Δx
CORRECT SAMPLE POSITION
90-θ
ψ = 0
ψ = ψ
PEAK SHIFT FROM ψ = 0 TO ψ = ψ

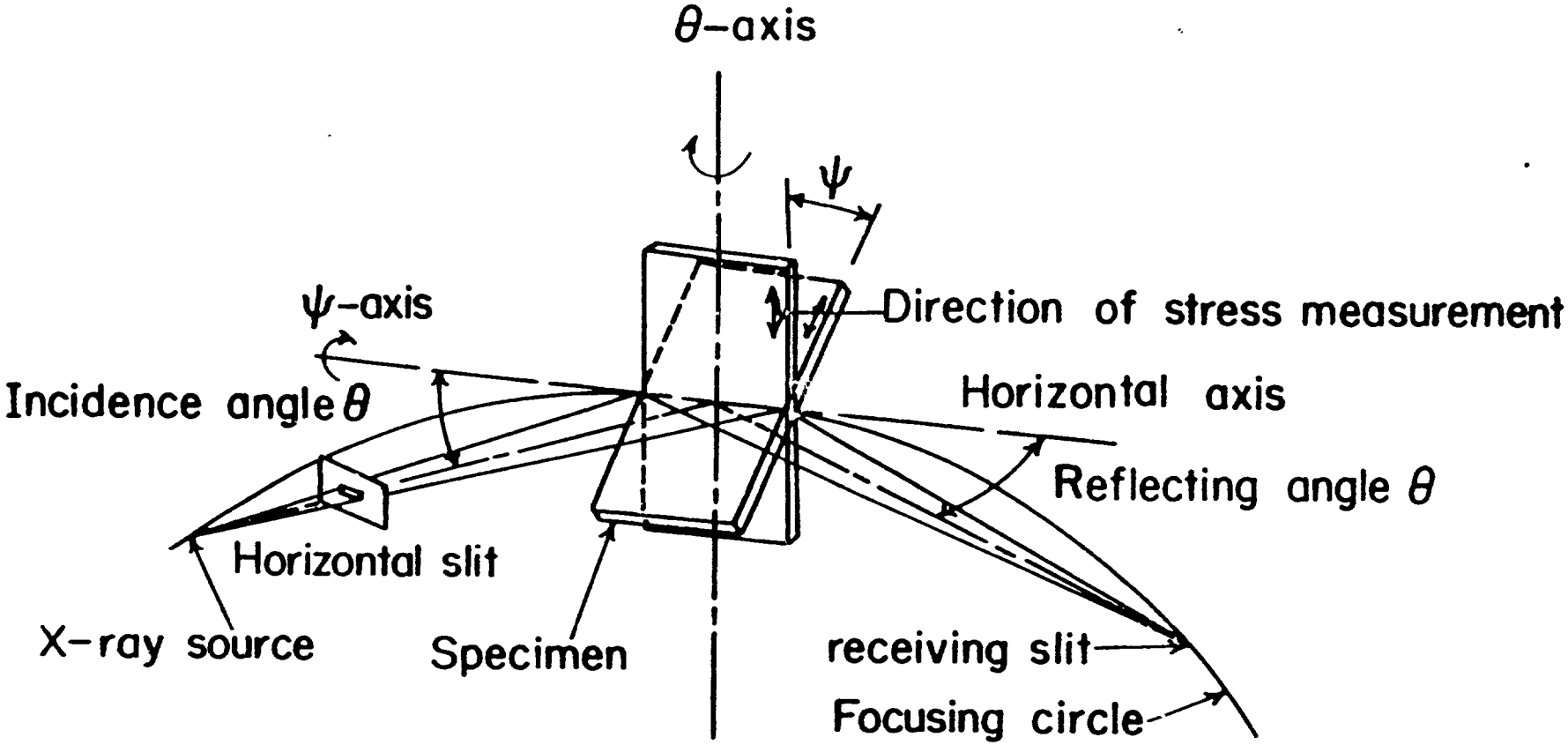
θ-axis
ψ
ψ-axis
Direction of stress measurement
Incidence angle θ
Horizontal axis
Reflecting angle θ
Horizontal slit
X-ray source
Specimen
receiving slit
Focusing circle

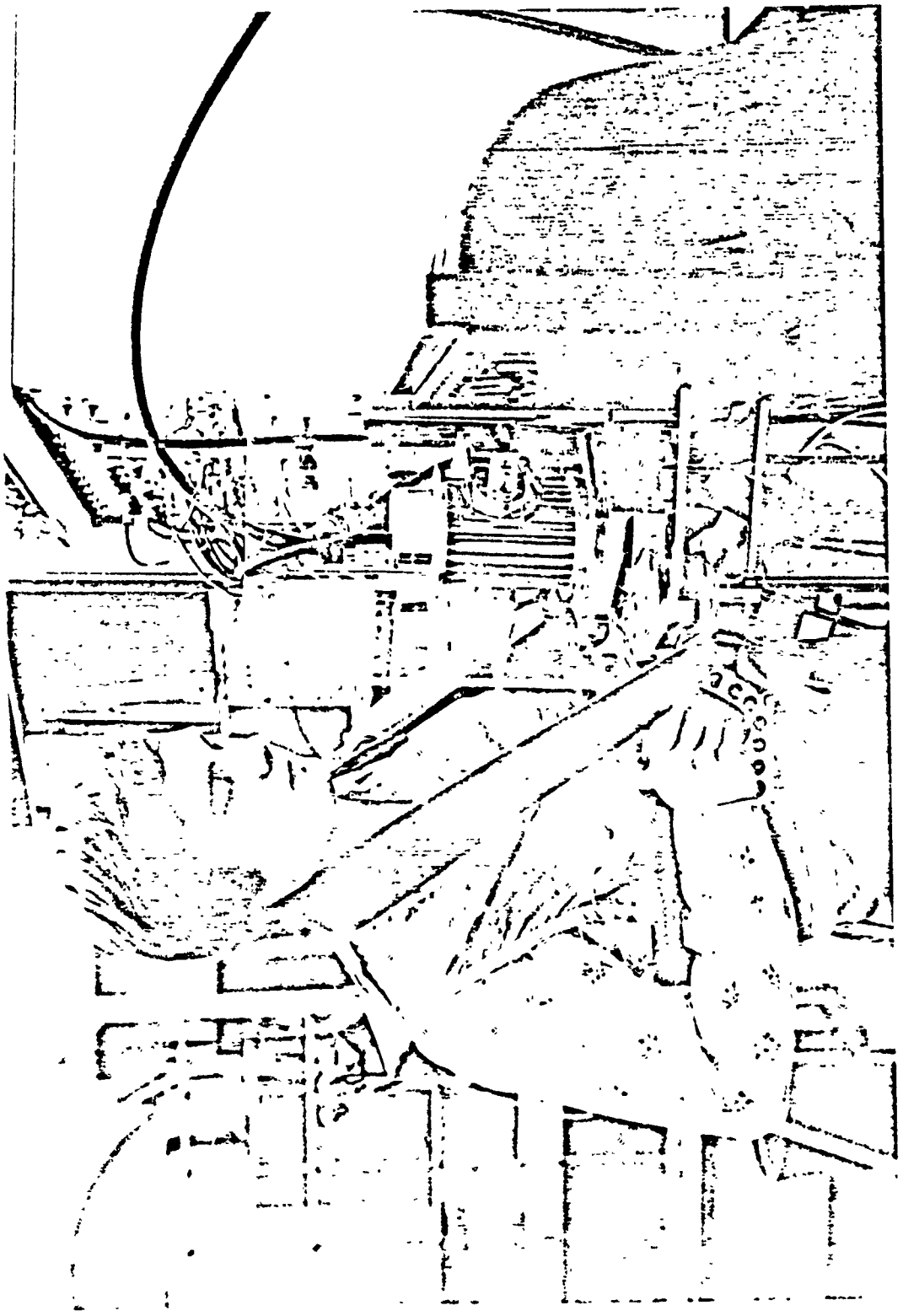

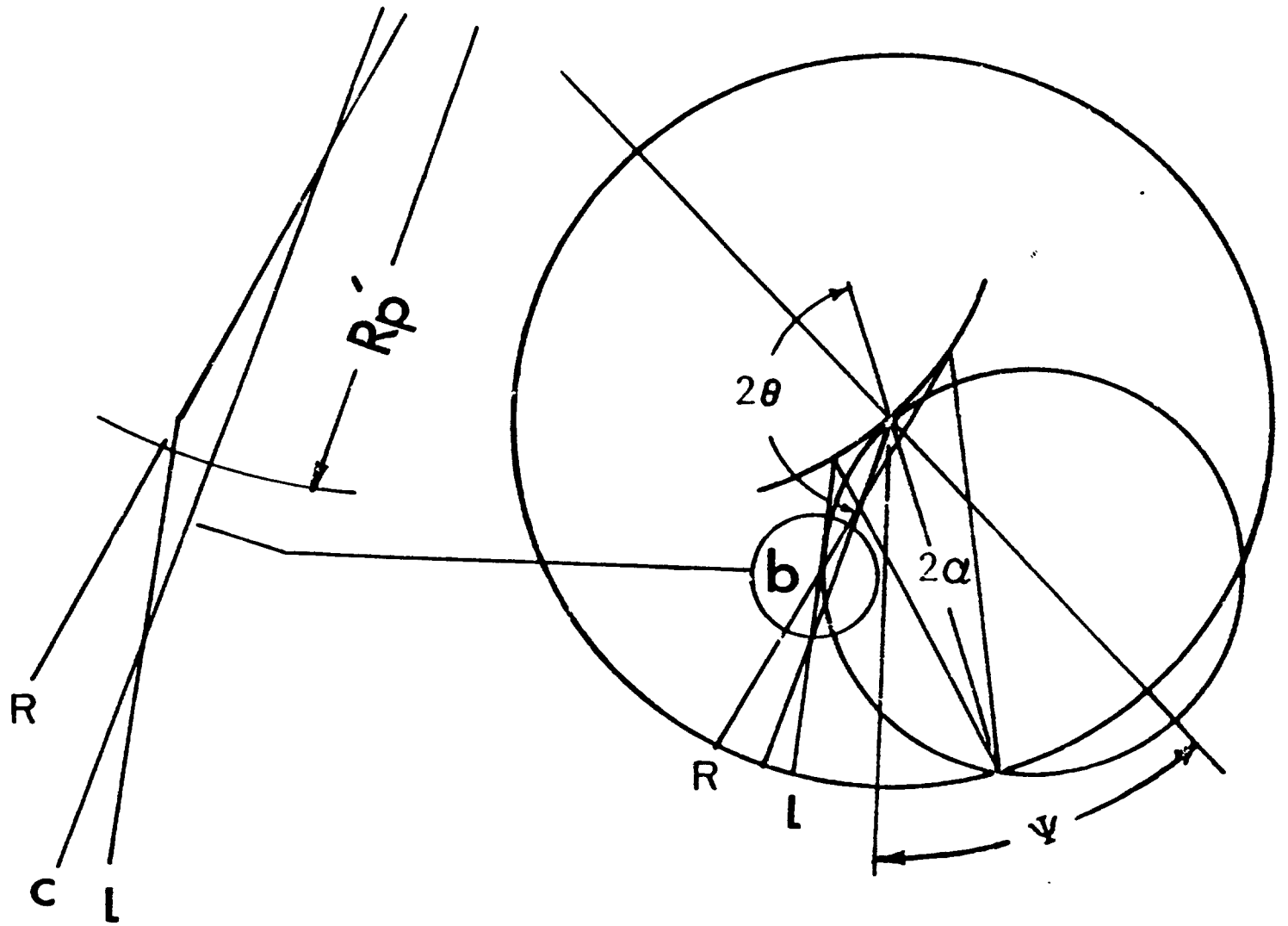

(b) (a)

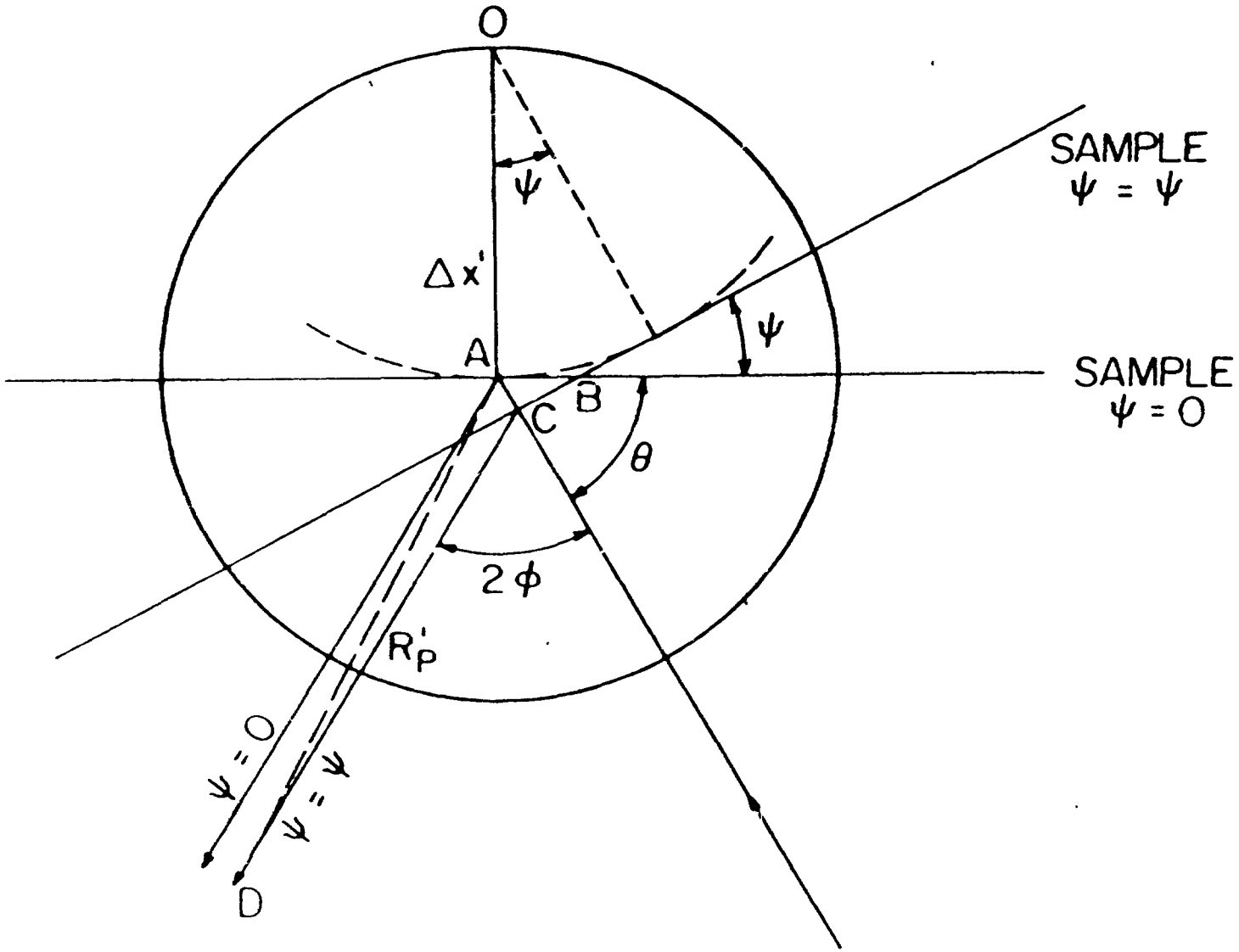
O
ψ
Δx'
A
SAMPLE
ψ = ψ
ψ
SAMPLE
ψ = 0
B
C
θ
2φ
R'P
ψ = 0
ψ = ψ
D

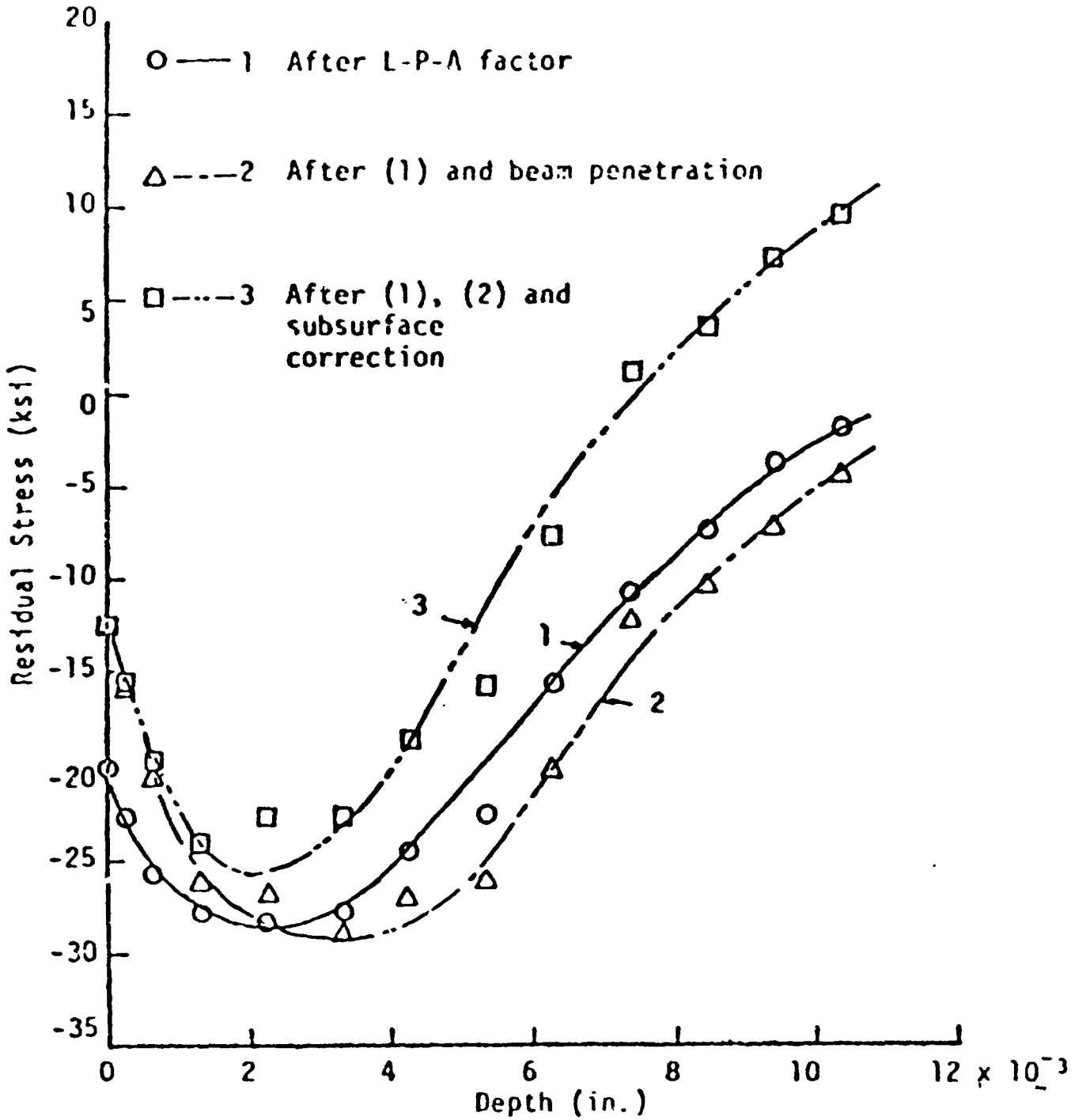
O—— 1 After L-P-A factor
△---2 After (1) and beam penetration
□-·-·-3 After (1), (2) and subsurface correction
Residual Stress (ksi)
20
15
10
5
0
-5
-10
-15
-20
-25
-30
-35
0
2
4
6
8
10
12 x 10⁻³
Depth (in.)
1
2
3

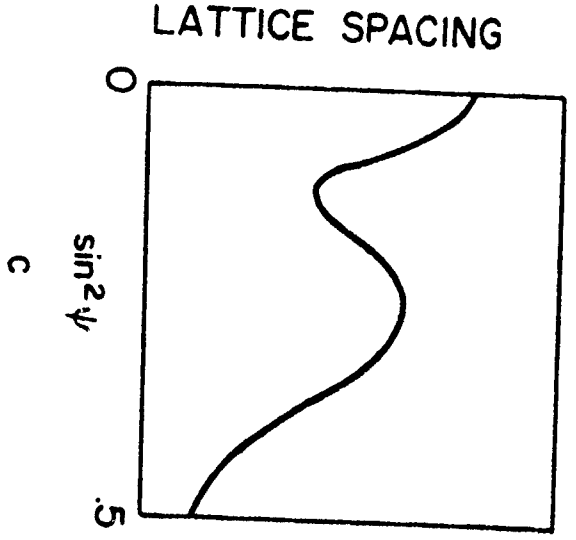
LATTICE SPACING
0
$\sin^2\psi$
.5
c

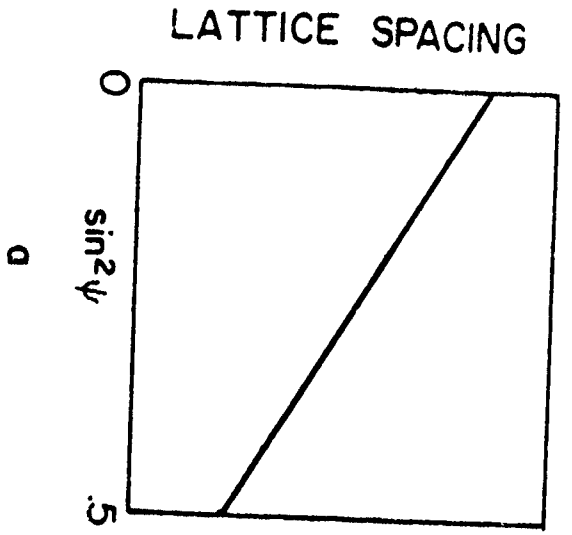
LATTICE SPACING
0
$\sin^2\psi$
.5
a

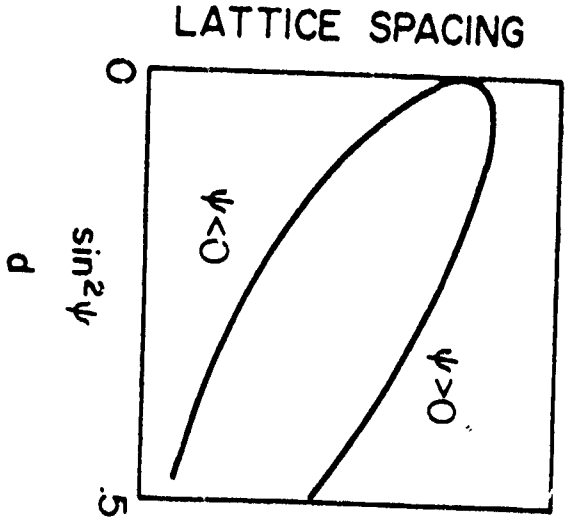
LATTICE SPACING
0
$\sin^2\psi$
.5
d
$\psi<0$
$0<\psi$

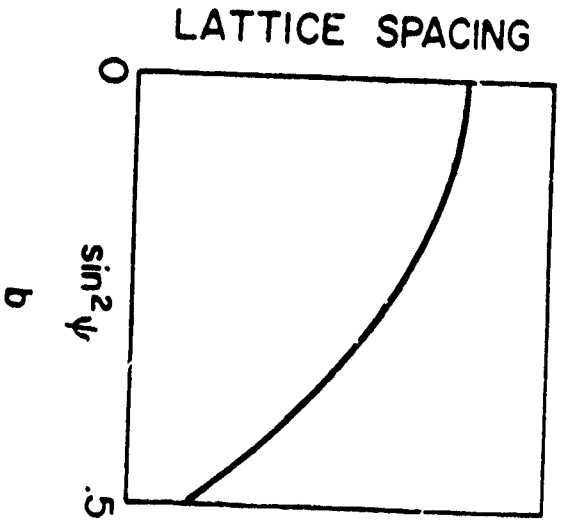
LATTICE SPACING
0
$\sin^2\psi$
.5
b

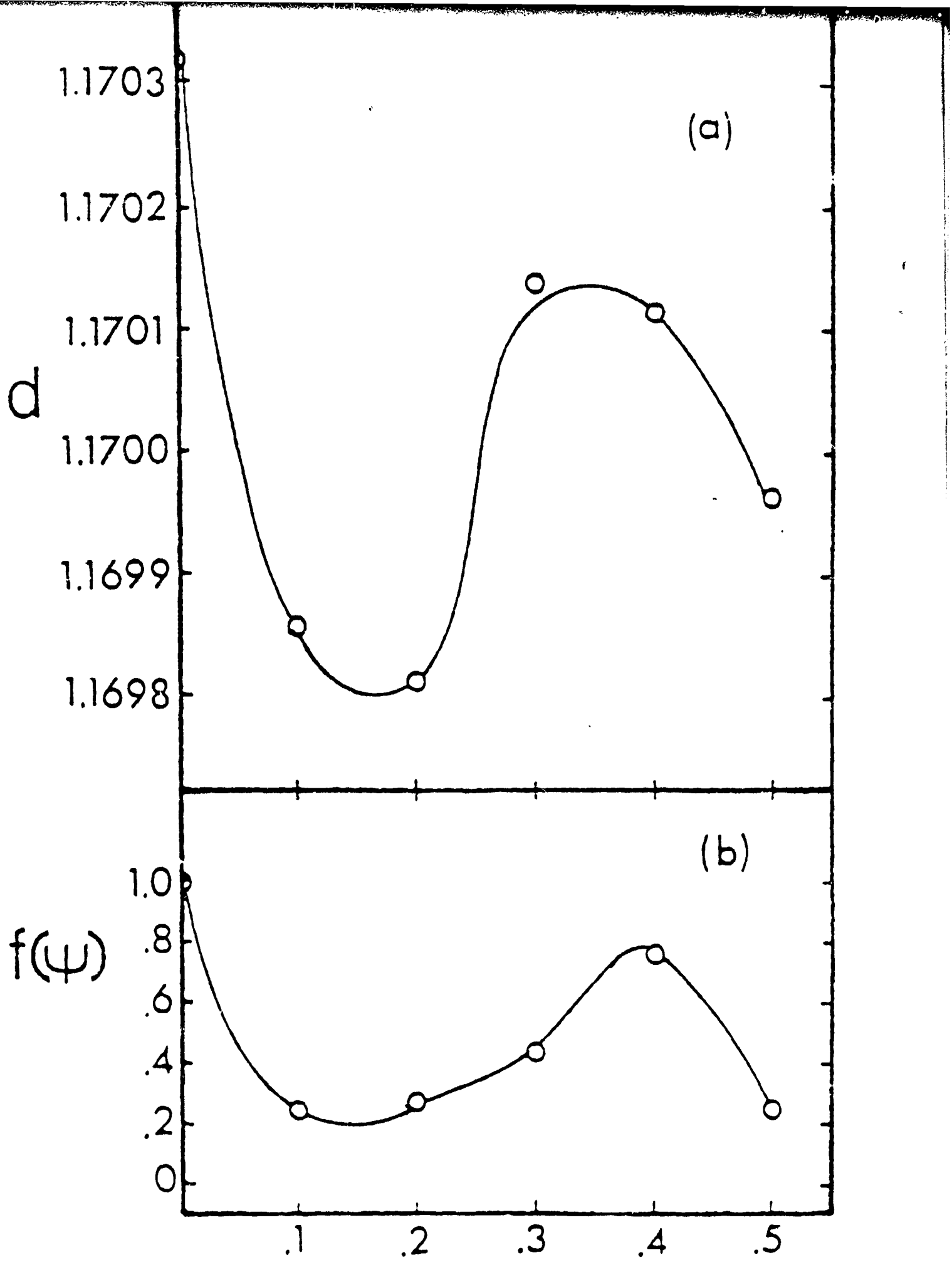
1.1703
1.1702
1.1701
1.1700
1.1699
1.1698
d
(a)
(b)
1.0
.8
.6
.4
.2
0
f(ψ)
.1
.2
.3
.4
.5

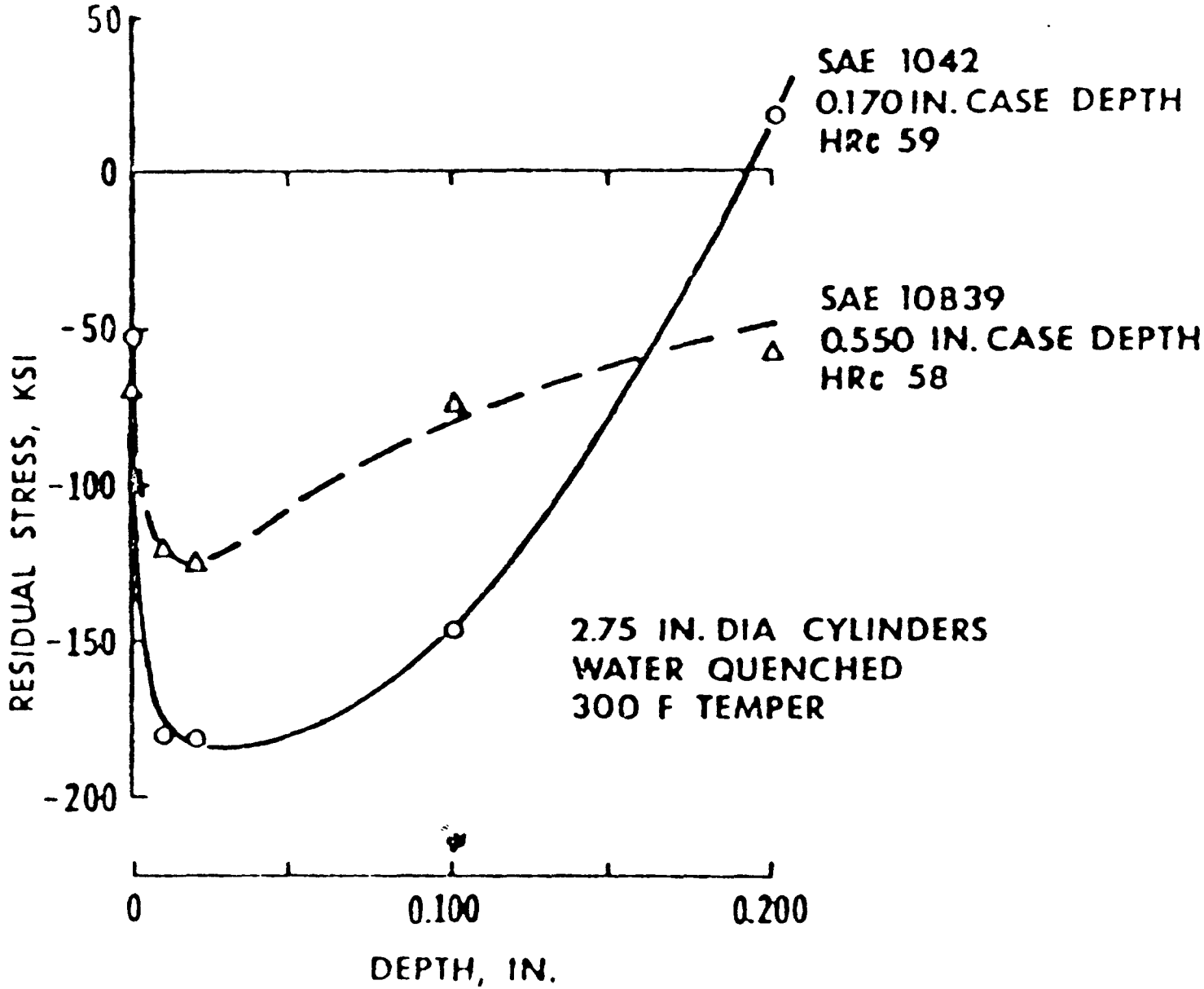
50
0
-50
-100
-150
-200
RESIDUAL STRESS, KSI
0
0.100
0.200
DEPTH, IN.
SAE 1042
0.170 IN. CASE DEPTH
HRc 59
SAE 10B39
0.550 IN. CASE DEPTH
HRc 58
2.75 IN. DIA CYLINDERS
WATER QUENCHED
300 F TEMPER

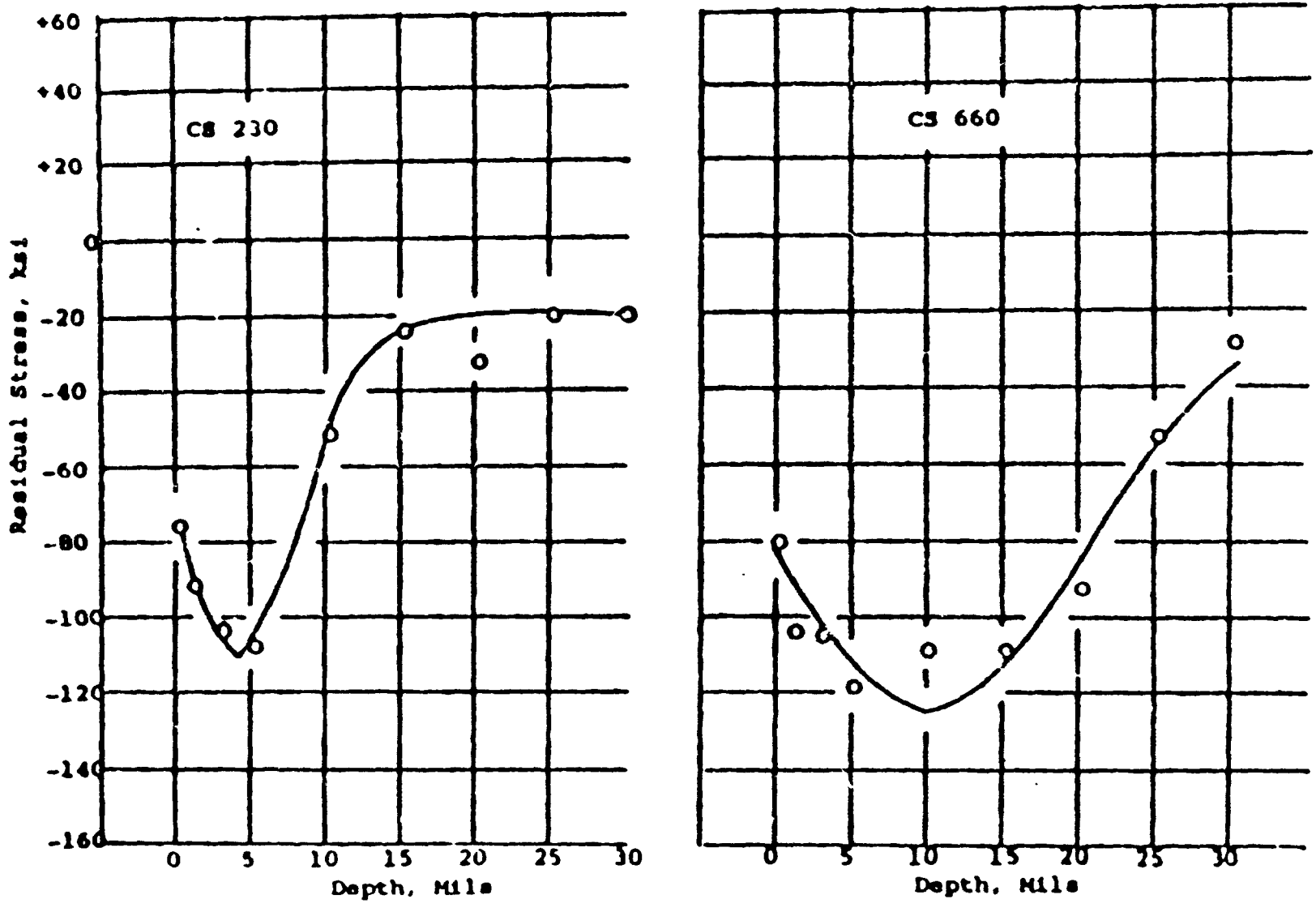
CS 230
CS 660
+60
+40
+20
0
-20
-40
-60
-80
-100
-120
-140
-160
Residual Stress, ksi
0
5
10
15
20
25
30
Depth, Mils

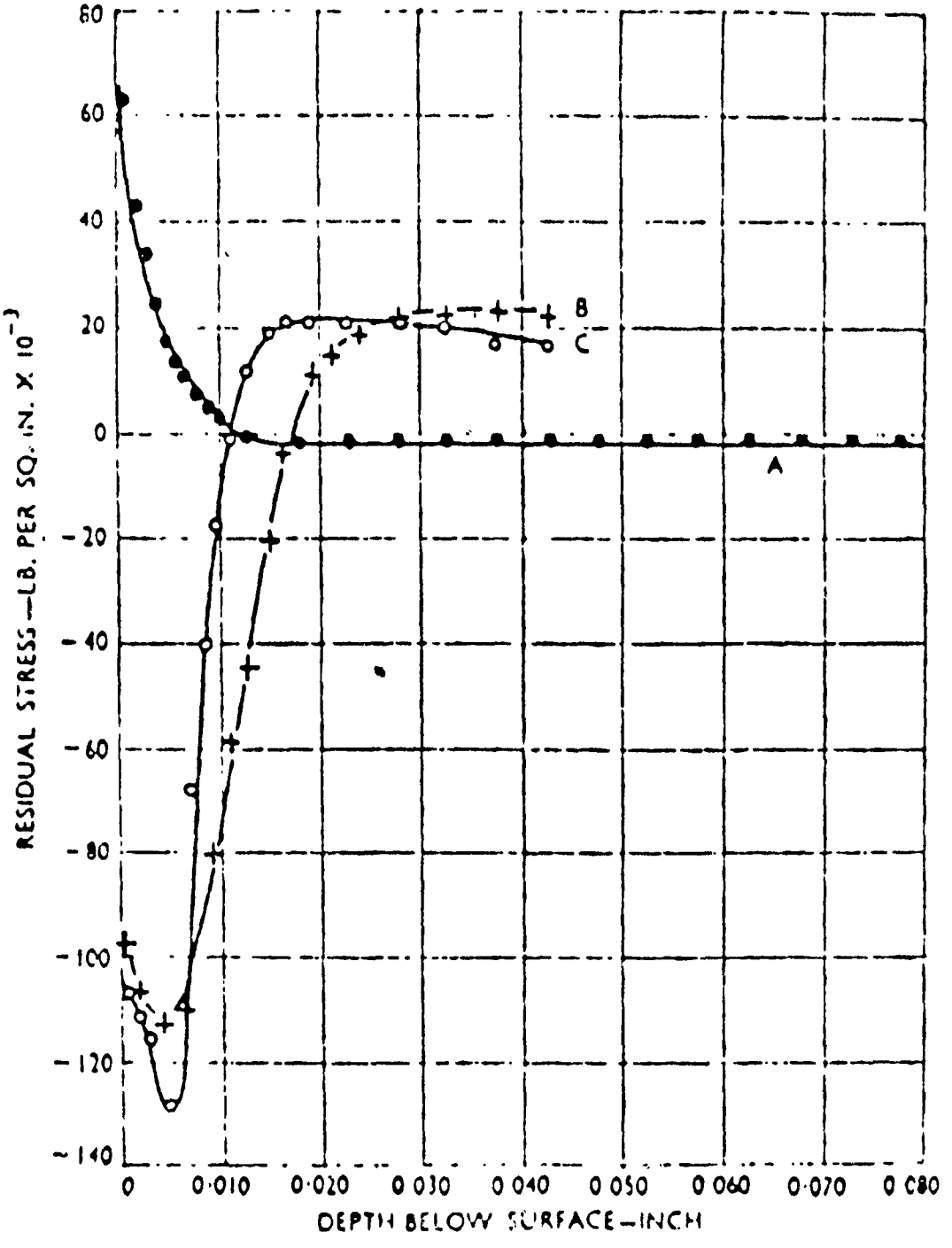
RESIDUAL STRESS—LB. PER SQ. IN. X 10^{-3}
60
40
20
0
-20
-40
-60
-80
-100
-120
-140
0
0·010
0·020
0 030
0 040
0 050
0 060
0·070
0 080
DEPTH BELOW SURFACE—INCH
A
B
C

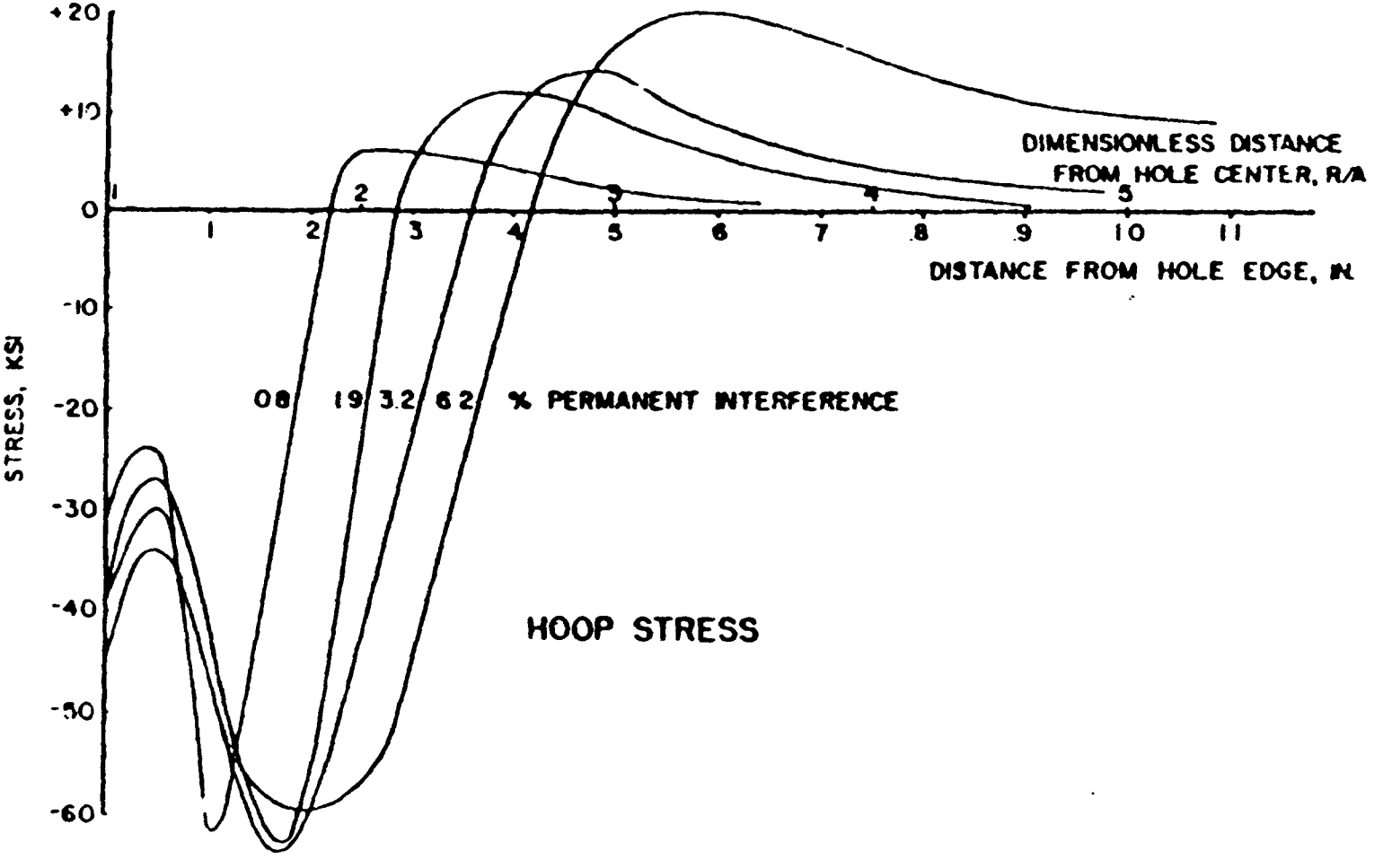
+20
+10
0
-10
-20
-30
-40
-50
-60
STRESS, KSI
1
2
3
4
5
6
7
8
9
10
11
DISTANCE FROM HOLE EDGE, IN.
DIMENSIONLESS DISTANCE
FROM HOLE CENTER, R/A
1
2
3
4
5
0.8
1.9
3.2
6.2
% PERMANENT INTERFERENCE
HOOP STRESS

Security Classification

DOCUMENT CONTROL DATA - R & D

(Security classification of title, body of abstract and indexing annotation must be entered when the overall report is classified)

1 ORIGINATING ACTIVITY (Corporate author)	2a. REPORT SECURITY CLASSIFICATION
J. B. Cohen, Northwestern University, Evanston, IL.	Unclassified
	2b. GROUP

3 REPORT TITLE

THE MEASUREMENT OF RESIDUAL STRESSES BY X-RAY DIFFRACTION TECHNIQUES

4. DESCRIPTIVE NOTES (Type of report and inclusive dates)
Technical Report No. 21

5 AUTHOR(S) (First name, middle initial, last name)

M. R. James and J. B. Cohen

6. REPORT DATE	7a. TOTAL NO. OF PAGES	7b. NO. OF REFS
N00014 - 75-C-0580 NR 031-733	107 pages	

8a. CONTRACT OR GRANT NO	9a. ORIGINATOR'S REPORT NUMBER(S)
5345-455	Technical Report No. 21
b. PROJECT NO	
c.	9b OTHER REPORT NO(S) (Any other numbers that may be assigned this report)
d.	None

10 DISTRIBUTION STATEMENT

Distribution of this document is unlimited.

11 SUPPLEMENTARY NOTES	12. SPONSORING MILITARY ACTIVITY
	Office of Naval Research, Metallurgy Branch

13 ABSTRACT

In this report the main aim is to present, in a single chapter, many of the recent instrumental advances and to explain the fundamental limitations associated with the measurement, in the hope of providing an insight into its proper application. In doing so, many current applications are described in those areas where the measurement has already proven to be useful.

DD FORM 1 NOV 65 1473 (PAGE 1)

S/N 0101-807-6801

Security Classification

14 KEY WORDS	LINK A		LINK B		LINK C	
	ROLE	WT	ROLE	WT	ROLE	WT
residual stresses, stresses, x-rays, diffraction						